CORA Cork Open Research Archive
Cartlann Taighde Oscailte Chorcaí

Title	Electroporation of a nanoparticle-associated DNA vaccine induces higher inflammation and immunity compared to its delivery with microneedle patches in pigs
Authors	Bernelin-Cottet, Cindy;Urien, Céline;McCaffrey, Joanne;Collins, Damien;Donadei, Agnese;McDaid, Dennis;Jakob, Virginie;Barnier-Quer, Christophe;Collin, Nicolas;Bouguyon, Edwige;Bordet, Elise;Barc, Céline;Boulesteix, Olivier;Leplat, Jean-Jacques;Blanc, Fany;Contreras, Vanessa;Bertho, Nicolas;Moore, Anne C.;Schwartz-Cornil, Isabelle
Publication date	2018-08-28
Original Citation	Bernelin-Cottet, C., Urien, C., McCaffrey, J., Collins, D., Donadei, A., McDaid, D., Jakob, V., Barnier-Quer, C., Collin, N., Bouguyon, E. and Bordet, E., 2019. Electroporation of a nanoparticle-associated DNA vaccine induces higher inflammation and immunity compared to its delivery with microneedle patches in pigs. Journal of Controlled Release. 308, pp. 14-28. DOI:10.1016/j.jconrel.2019.06.041
Type of publication	Article (peer-reviewed)
Link to publisher's version	https://www.sciencedirect.com/science/article/pii/S0168365919303840 - 10.1016/j.jconrel.2019.06.041
Rights	© 2019 The Authors. Published by Elsevier B.V. This is an open access article under the CC BY-NC-ND license - https://creativecommons.org/licenses/by-nc-nd/4.0/
Download date	2026-11-02 11:10:27
Item downloaded from	https://hdl.handle.net/10468/8925



University College Cork, Ireland
Coláiste na hOllscoile Corcaigh

Journal of Controlled Release 308 (2019) 14–28

Contents lists available at ScienceDirect

Journal of Controlled Release

journal homepage: www.elsevier.com/locate/jconrel

Electroporation of a nanoparticle-associated DNA vaccine induces higher inflammation and immunity compared to its delivery with microneedle patches in pigs

Cindy Bernelin-Cottet[a], Céline Urien[a], Joanne McCaffrey[b,c], Damien Collins[b,c], Agnese Donadei[b,c], Dennis McDaid[c], Virginie Jakob[d], Christophe Barnier-Quer[d], Nicolas Collin[d], Edwige Bouguyon[a], Elise Bordet[a], Céline Barc[e], Olivier Boulesteix[e], Jean-Jacques Leplat[f], Fany Blanc[f], Vanessa Contreras[g], Nicolas Bertho[a,h], Anne C. Moore[b,*,1], Isabelle Schwartz-Cornil[a,*,1]

[a] VIM, INRA, Université Paris-Saclay, Domaine de Vilvert, 78350 Jouy-en-Josas, France
[b] School of Pharmacy, School of Biochemistry and Cell Biology, University College Cork, Cork, Ireland
[c] Xeolas Pharmaceuticals Ltd., Dublin, Ireland
[d] Vaccine Formulation Laboratory, University of Lausanne, Chemin des Boveresses 155, 1066 Epalinges, Switzerland
[e] PFIE-UE1277, INRA, 37380 Nouzilly, France
[f] GABI, INRA-AgroParisTech, Université Paris-Saclay, Domaine de Vilvert, 78350 Jouy-en-Josas, France
[g] Immunology of viral infections and autoimmune diseases, IDMIT Department, IBFJ, INSERM U1184-CEA - Université Paris Sud 11, Fontenay-Aux-Roses et Le Kremlin-Bicêtre, France
[h] BIOEPAR, Oniris, INRA, 44307 Nantes, France

ARTICLE INFO

Keywords:
DNA vaccines
Skin
Pig model
Dissolvable microneedle
Electroporation
PLGA nanoparticles

ABSTRACT

DNA vaccination is an attractive technology, based on its well-established manufacturing process, safety profile, adaptability to rapidly combat pandemic pathogens, and stability at ambient temperature; however an optimal delivery method of DNA remains to be determined. As pigs are a relevant model for humans, we comparatively evaluated the efficiency of vaccine DNA delivery in vivo to pigs using dissolvable microneedle patches, intradermal inoculation with needle (ID), surface electroporation (EP), with DNA associated or not to cationic poly-lactic-*co*-glycolic acid nanoparticles (NPs). We used a luciferase encoding plasmid (pLuc) as a reporter and vaccine plasmids encoding antigens from the Porcine Reproductive and Respiratory Syndrome Virus (PRRSV), a clinically-significant swine arterivirus. Patches were successful at inducing luciferase expression in skin although at lower level than EP. EP induced the cutaneaous recruitment of granulocytes, of $MHC2^{pos}CD172A^{pos}$ myeloid cells and type 1 conventional dendritic cells, in association with local production of IL-1β, IL-8 and IL-17; these local responses were more limited with ID and undetectable with patches. The addition of NP to EP especially promoted the recruitment of the $MHC2^{pos}CD172A^{pos}$ $CD163^{int}$ and $CD163^{neg}$ myeloid subsets. Notably we obtained the strongest and broadest IFNγ T-cell response against a panel of PRRSV antigens with DNA + NPs delivered by EP, whereas patches and ID were ineffective. The anti-PRRSV IgG responses were the highest with EP administration independently of NPs, mild with ID, and undetectable with patches. These results contrast with the immunogenicity and efficacy previously induced in mice with patches. This study concludes that successful DNA vaccine administration in skin can be achieved in pigs with electroporation and patches, but only the former induces local inflammation, humoral and cellular immunity, with the highest potency when NPs were used. This finding shows the importance of evaluating the delivery and immunogenicity of DNA vaccines beyond the mouse model in a preclinical model relevant to human such as pig and reveals that EP with DNA combined to NP induces strong immunogenicity.

* Corresponding authors.
E-mail address: isabelle.schwartz@inra.fr (I. Schwartz-Cornil).
[1] Anne C. Moore and Isabelle Schwartz-Cornil are senior authors and corresponding authors.

https://doi.org/10.1016/j.jconrel.2019.06.041
Received 6 May 2019; Received in revised form 26 June 2019; Accepted 28 June 2019
Available online 29 June 2019
0168-3659/ © 2019 The Authors. Published by Elsevier B.V. This is an open access article under the CC BY-NC-ND license (http://creativecommons.org/licenses/BY-NC-ND/4.0/).

1. Introduction

Nucleic acid-based vaccine strategies are attractive technologies as they present a good safety profile due to lack of infectious risk, they are amenable to rapid, standardized and cost-effective manufacturing processes, and due to their ease of manipulation, they are adaptable to emerging pandemic pathogen strains. While RNA vaccines show high promises due to recent improvement in synthetic mRNA production and stability [1,2], DNA vaccines remain an important technology [2–4], considering their good tolerance and safety profile from numerous clinical trial results, their efficacy in recent human studies [5–8], the validated high-scale production mode favoring competitive cost, the existence of five commercialized DNA veterinary vaccines [9,10] and the high stability outside of the cold chain, an important property for use in tropical low- and middle-income countries where vaccine need is particularly high [11]. In the last decade, new developments have improved the DNA vaccine immunogenicity and safety profiles, by optimizing the DNA constructs, targeting vaccine antigens to dendritic cells, providing adjuvant sequences, and importantly, by improving the DNA delivery to promote the crossing of the cell and nucleus membrane taking into account ease of administration and acceptability [2–4]. Among the vaccine DNA delivery methods, electroporation (EP) appears to have generated the biggest advance in the field [10,12,13]: the applied current induces pores in the cell membrane and directs the DNA through the cell towards the positive electrode, and the local inflammation, possibly elicited by cell damage, has been associated to the induction of adaptive immune responses in different species including mice, pigs and non-human primates [14–17]. Importantly, different EP devices have been developed to deliver the DNA in muscle and skin with good results in preclinical models and in clinical trials [10]. The immuno-competence of the skin with its richness in antigen-presenting cells and dermal lymphatic vessels, as well as its easy access, make skin an organ of choice for DNA vaccine delivery. In addition, EP can be performed at the skin surface and is less invasive and painful as compared to in muscle [13,17]. Yet, EP is coupled to delivery by needle in skin and it induces discomfort and pain; therefore, other methods, based on different types of microneedles, have been developed. Microneedles are sharp micro-projections that pierce the stratum corneum and deliver vaccines and drugs into skin, without stimulating pain receptors or affecting blood vessels. Different microneedle patch designs for DNA delivery include solid [18], coated [19], and lately, dissolvable microneedles [20,21]. These microneedle-based methods were shown to be efficient at promoting gene transfer, expression of antigens, and immune responses in mouse models [18–21]. However, very few studies document the potency of DNA vaccines delivered by microneedle patches in larger species [22,23] despite the demonstration of efficient material and gene transfer in ex vivo cadaver skin [24,25]. To our knowledge, no studies have examined the immunogenicity of DNA vaccines delivered by microneedle patches to pigs. Dissolvable microneedle patches incorporate the vaccine in their matrix that they release after skin insertion due to dissolution of the microneedle in the hydrated skin tissue, and they are fully biocompatible, stable and easy to use [21,26]. Interestingly, one of our recent studies showed that dissolvable microneedle patches with incorporated trivalent inactivated influenza vaccine elicited higher and broader immunity compared to intramuscular injection in mice [27]. In the case of DNA delivery with dissolvable microneedles, CTL and B cell responses were induced against papillomavirus antigens in mice [21]. However, the studies with DNA delivered by microneedle patches were performed in the mouse model and, although promising, they do not preclude that similar results would be obtained in larger species. Pigs are the most appropriate animal model for human skin [28] as pig skin shares structural and histological features with human skin, and we previously described similarities in the composition of mononuclear phagocyte subsets [29]. Therefore, pig is a highly relevant preclinical model for assessments of DNA vaccine delivery strategies in skin both for translation to human and possible veterinary application for improving livestock health and welfare.

In this study, we comparatively evaluated different delivery methods of DNA vaccines in the pig for their efficacy in gene transfer and immunogenicity. The methods are dissolvable microneedle patches loaded with DNA (thereafter designated as patches), simple intradermal (ID) inoculation with needle and surface EP. The DNA vaccine encoded antigens from a pig arterivirus, the porcine reproductive and respiratory virus (PRRSV) which is the most damaging virus in swine worldwide [30]. The plasmid DNA was used either as a naked plasmid or coated on cationic poly-lactic-*co*-glycolic acid (PLGA) nanoparticles (NPs), which were previously shown to promote DNA vaccine efficacy in mice when coupled to microneedles [31] or even to EP [32]. Previous studies indicated that DNA vaccine immunogenicity results from the combined effect of gene expression efficiency and local responses, which are induced by the delivery method as electrical pulses applied prior to intradermal injection promoted the immune response [16,32]. Therefore, we also evaluated the gene transfer efficiency and the local inflammation induced by surface EP, simple ID and patches with DNA combined or not to cationic PLGA NPs in order to get insight into the parameters involved in immunogenicity. Altogether we found that all delivery methods, i.e. patches, ID and EP, induced skin cell transfection. EP, especially when combined to cationic PLGA NPs, triggered substantial anti-PRRSV B and T cells responses whereas ID only induced low antibody responses and patches did not induce significant response. These adaptive responses were associated to local skin responses with myeloid cell subsets and granulocyte recruitment and cytokine production, and suggest that patches lack an immuno-adjuvant effect.

2. Materials and methods

2.1. Antibodies

The anti-pig IFNγ mouse P2G10 mAb (capture) and biotinylated anti-pig IFNγ P2G11 mAb were from MabTech AB (Nacka Strand, Sweden). The anti-pig IgA mouse mAb K61−1B4 was bought from Bio-Rad Antibodies. The anti-pig MHC class II mAb (mouse IgG2a, clone MSA3), anti-CD172a (mouse IgG2b, clone 74–22–15a) were purchased from the mAb Center Washington State University (USA). The in-house produced anti-pig CD13 mAb (mouse IgG1, clone T35) were purified from mouse ascites using protein A chromatography [33]. The biotinylated mAb anti-human langerin (rat IgG2a, clone 929F3) was obtained from Dendritics (France). Irrelevant unconjugated mouse IgG1, IgG2a and IgG2b, biotinylated rat IgG2a, Alexa 488-conjugated mouse IgG2a and PE-conjugated mouse IgG1 (Bio-Rad Antibodies) were used as isotype controls. The anti-6xHis rabbit polyclonal IgG was purchased from Abcam. The phycoerythrin (PE)-conjugated anti-CD163 mAb (mouse IgG1, clone 2A10/11), Alexa 488 (A488)-conjugated anti-granulocytes (mouse IgG2a, clone 6D10) and A488-streptavidin were bought from Bio-Rad Antibodies. A647-conjugated goat anti-rabbit IgG were bought from Jackson ImmunoResearch (USA). A647-conjugated goat anti-mouse (GAM) IgG2a, EF710 PerCP5.5-conjugated GAM IgG1 and APC-Cy7-conjugated GAM IgG2b were purchased from Fisher Scientific. The horseradish peroxidase (HRP)-conjugated anti-rabbit antibody was purchased from Sigma-Aldrich and the HRP-conjugated rat anti-mouse IgG1 from BD-bioscience.

2.2. Preparation of cationic poly-lactic-co-glycolic acid (PLGA) nanoparticles (NPs) and coating with DNA

The NPs were prepared as follows: the PLGA RG502H polymer (Sigma), was dissolved in methylene chloride as a 5% (*w/v*) solution and 1 ml was emulsified with 0.1 ml of Tris 5 mM pH 7.4 at high speed using a probe sonicator. The primary emulsion was then added to 5 ml of distilled water containing cetyltrimethylammonium bromide (CTAB) (0.5%, w/v). The resulting PLGA-CTAB nanoparticles were washed

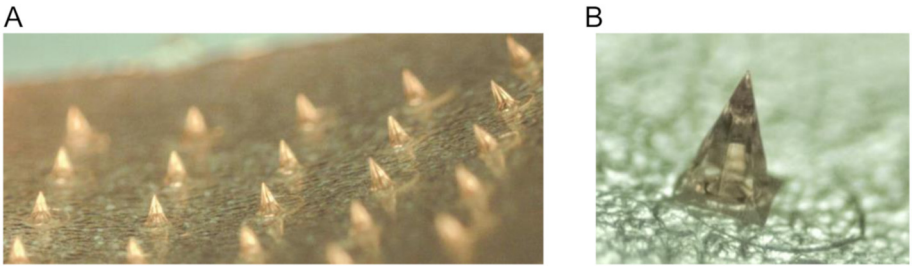


Fig. 1. DNA-loaded dissolvable microneedle patches. (A). An image of the array of needles. Each patch was 9 cm^2 and comprised of 225 microneedles. (B). An image of a single microneedle that is 500 μm in height and has a base of 333 μm diameter. DNA was loaded throughout the entire microneedle.

once in buffer by centrifugation at 10,000*g*. After preparation, washing, and collection, DNA was adsorbed onto the nanoparticles. After optimization, NP:DNA were combined at a 1:20 (μg/μg) ratio for all formulations.

2.3. Production of dissolvable microneedle patches

Dissolvable microneedle patches contained 225 microneedles in a 9 cm^2 area (Fig. 1). They were prepared as previously described [27]. DNA (400 μg) was loaded in 73 μl of formulation comprised of 11% (*w/v*) trehalose and 1.25% (w/v) polyvinyl alcohol (PVA) as excipients (5.5 mg/ml DNA concentration). Formulation was delivered directly onto water-filled microneedle cavities in a polydimethylsiloxane (PDMS) mould at a rate of 1–3 μl/min. Formulation in the moulds was dried overnight at room temperature and then pulled from the mould onto medical grade adhesive tape (1525 L-Poly-Med tape, 3 M). A scoring system was used to grade the physical quality of 1 cm^2 patch units; a patch with a score of 100 reflected a patch where all 25 microneedles per 1cm^2 were perfectly formed. A score of 92 (maximum of 2 missing microneedles) per 1 cm^2 was set as the lower limit of acceptability. The total dose of DNA plasmid, with and without NPs, per patch, set to 400 μg, was assessed by nanodrop. The quality of the plasmid in the patches compared to the liquid stock was determined by agarose gels.

2.4. Construction and production of plasmids

The plasmid encoding porcine GM-CSF (pGM-CSF) has been previously described [34]. A mCherry encoding plasmid (pmCherry2-N1, here referred to pmCherry) was obtained from Addgene under MTA. A firefly luciferase expression plasmid (pLuc) was kindly provided by Stéphane Biacchesi (INRA, France). The pLuc plasmid includes the eGFP and firefly luciferase sequences separated by a viral IRES cloned in a pcDNA3.1 expression vector. pcDNA3.1 vectors encoding for four PRRSV antigen (PRRSV-AG) sequences from the 13 V091 isolate were synthetized by GeneArt. The antigen sequences were i) a GP4GP5M chimera that was derived from [35] and transposed to the 13 V091 viral sequence (1008 nt), ii) NSP1β (1176 nt), iii) RdRp (1962 nt), and iv) N (405 nt). In the case of NSP1β and RdRp which are naturally synthetized from viral polyprotein precursors (ORF1 and 2), an exogenous kozak sequence was added. Only GP4GP5M is expected to be secreted as it includes the natural leader peptide of GP4. Each antigen sequence was terminated by a 6xHis tag. The plasmids are named pGP4GP5M, pN, pNSP1β, and pRdRp. Plasmid productions for immunization were prepared using Endofree® Plasmid Giga Kits (Qiagen) according to the manufacturer's instructions and were stored at −20 °C until use.

2.5. Plasmid transfection in vitro

293 T cells were cultivated in DMEM +10% fetal calf serum (FCS). 293 T cells (1.8×10^5) were plated and transfected in P12-well plates with 1 μg of each PRRSV-AG coding plasmid, with a control pcDNA3.1 plasmid encoding for an irrelevant antigen (pcDNA3.1-ctrl), and a marker plasmid (pmCherry, transfection control) using Fugene HD (Roche), according to the manufacturer recommendations. After 2 days, cells were harvested and processed for detection of expressed antigen by immunofluorescence or Western blot.

2.6. Cell lysate and western blots

Transfected 293 T cells from 2 transfected P12-well plates were lysed in RIPA buffer 150 mM sodium chloride, 1.0% Triton X-100, 0.5% sodium deoxycholate, 0.1% SDS, 50 mM Tris, 5 mM EDTA and a protease inhibitor cocktail, pH 8.0 at 4 °C. Protein dosage was done with a Bradford assay against a bovine serum albumin (BSA) standard in RIPA. Cell lysates (5 μg) were analyzed by Western Blot following a 12% SDS-PAGE under reducing conditions. Blots were washed with PBS + 0.05% Tween 20 and incubated overnight at 4 °C with anti-6xHis rabbit IgG at a 1:5000 dilution in PBS + 3% BSA + Tween 0.3% (*w/v*) followed by HRP-conjugated anti-rabbit antibody at a 1:100000 dilution in PBS + 3% BSA + Tween 0.3% overnight at 4 °C. Immuno-reactive bands were visualized with the Clarity Western ECL Substrate (Bio-Rad) according to the manufacturer's protocol. Image acquisitions were done with Chemidoc imaging system (Bio-Rad).

2.7. Pig studies

The experiments with the pLuc plasmid (skin cell transduction and local inflammation) were approved by the COMETHEA ethic committee under the number 13195–2017120408328722 v2 in accordance with national guidelines on animal use and performed at the Animal Genetics and Integrative Biology unit (GABI-INRA), France, under the accreditation number for animal experimentation C78–719. Large White pigs (9 pigs, 10 weeks of age) were obtained from INRA UEPR Rennes-Saint Gilles. The immunization experiments with PRRS-AG encoding plasmids was approved by the Comité d'Éthique en Expérimentation Animale Val de Loire under the number 15051418327338 v10 and were done at the Plate-forme d'Infectiologie Expérimentale PFIE-INRA, Nouzilly, France (https://doi.org/10.15454/1.5535888072272498e12) under the accreditation number for animal experimentation C37–1753 in a A-BSL1 containment. Large White pigs (46 pigs with 5 for EP optimization and 41 for immunogenicity, 4-week-old) were obtained from the INRA conventional breeding unit Unité Expérimentale de Physiologie Animale de l'Orfrasière PAO-INRA, Nouzilly, France. A first experiment with pLuc plasmid on myeloid cell recruitment and luciferase expression (data not shown) was conducted on 6 pigs at PFIE-INRA, under the 15,051,418,327,338 v10 authorization, which gave similar results as the one reported here.

2.8. In vivo plasmid transfection for assessment of vector expression and local inflammation in pig skin

Pigs were anesthetized (2% isofluorane) to avoid animal discomfort with electroporation (EP) and to optimally control the quality of

vaccine administration. Pig skin in the inguinal zone for surface EP, in the ventral area for ID and in the lower thoracic zone for patch application was cleaned with Vetedine soap (Vetoquinol), washed and dried. The pLuc patches (9 cm^2, 400 μg DNA, plain DNA or adsorbed on cationic PLGA NPs) were placed on the skin under a 20 N force pressure for one minute. The pig flanks were then wrapped with Elastoplast to permit the maintenance of the patches on the skin for 24 h. For surface EP, intradermal injection of pLuc (in 100 μl saline, plain or adsorbed on NPs) was done in the inguinal zone and EP was performed on the site of injection using the CUY 21 EDIT system (NEPA Gene, Japan). For ID, intradermal injections were done in the ventral area. When stated, pGM-CSF was combined to pLuc (20 μg and 80 μg respectively). Disk electrodes (10 mm) were loaded with conductive gel (Alcyon, France) and 6 electric pulses were applied during 10 ms with 90 ms interval. Trolamine 0.6% (Biafine, France) was spread on the transfected zone right after administration.

Three groups of 3 pigs were used and designated as group 1, group 2 and Group 3. Group 1 (#4829, 896, 758) received pLuc + pGM-CSF or pLuc-only in EP and ID injections, Group 2 (#829, 850, 910) received pLuc-only in patches and EP, Group 3 (#878, 866, 925) received pLuc + pGM-CSF in patches. After 24 h, pigs were euthanized and skin biopsies were collected using an 8-mm diameter disposable biopsy punch (Kai medical, Japan) after cleaning of the skin with Vetedine soap and Vetedine 10% solution. Control skin was harvested from the same zone (inguinal for the EP, ventral for ID, and thoracic zone for the patches). For evaluation of transfection efficiency, each biopsy was cut into small pieces and lysed with 150 μl of lysis reagent (Luciferase Assay System E1500, Promega). Bioluminescence was measured per each biopsy using the In Vivo Imaging System (IVIS-200, Xenogen, UK) after adding 100 μl luciferin substrate. A region of interest (ROI) was manually selected and the intensity of luminescence (photons/s/cm^2) was recorded. For cytokine production assessment, each biopsy was carefully washed in PBS and placed in RPMI +10% FCS + 1% antibiotic/antimycotic cocktail for 24 h. For assessment of inflammatory cell mobilization, 6 biopsies were collected per condition, washed in PBS, pooled, minced and digested overnight in 6 ml RPMI +10% FCS + collagenase D (1 mg/ml, Roche) + dispase (0.5 mg/ml, InVitrogen) + DNAse (0.5 mg/ml, InVitrogen), + antimycotic antibiotic cocktail. The skin fragments were gently grinded with a 5 ml plunger through a metal wire mesh and the cell suspension was finally filtered through 100-μm and 40-μm pores-nylon mesh filters. For histology, skin biopsies from control skin, patch, EP and EP + NP DNA delivery sites from 3 pigs were fixed in 4% neutral-buffered formaldehyde and routinely processed and embedded in paraffin. Consecutive 4 μm thick sections were cut (3 per block), stained with hematoxylin-eosin-saffron (HES) and imaged using the caseviewer software (Sysmex-France, Villepinte, France).

In order to evaluate the voltage per cm (V/cm) parameter leading to optimal transfection in pig skin, the injected skin areas were subjected to EP with escalating pulses from 0 to 830 V/cm. in that case, skin was collected after 48 h. The optimal V/cm was 670 V/cm and was used in all subsequent experiments (supplementary material 1).

2.9. Staining of cells and flow cytometry analysis

Skin cells from skin biopsy extractions were washed in PBS. A skin cell fraction was processed for viable cell counts and debris exclusion using the Guava ViaCount assay and the GuavaSoft module (EMD Millipore Corporation); this method allowed us to determine the total cell counts per 6 biopsies. The rest of the skin cells were labeled with live/dead fixable dead cell kit (405 nm, In Vitrogen). Next, they were saturated in PBS supplemented with 5% horse serum and 5% pig serum for 30 min and labeled with a mix of primary monoclonal antibodies (mAb, 2 μg/ml) for 30 min, i.e. anti-MHC class II + anti-CD172a + anti-CD13 mAbs followed by EF710-PerCP5.5-conjugated GAM IgG1 + A647-conjugated GAM IgG2a + APC-Cy7-conjugated GAM IgG2b. After washing, secondary antibodies were saturated by an excess of mouse IgG1 and IgG2a (50 μg/ml) and finally labeled with PE-conjugated anti-CD163 and A488-conjugated anti-pig granulocytes mAb. Appropriate isotype control mAbs were used for fluorescence minus one controls. In order to detect intracellular langerin, cells were labeled as described above with anti-MHC class II + anti-CD172a mAbs followed by their conjugates, and finally with PE-conjugated anti-CD163 mAb. After wash, they were fixed and permeabilized using the Cytofix and Cytoperm kit (Becton Dickinson), and further incubated with biotinylated anti-langerin or control biotinylated isotype and finally with A488-streptavidin.

To test the proper expression of the plasmid-coding His-tagged antigens, 293 T cells were harvested after 48-h transfection in 2 mM EDTA and fixed and permeabilized using the Cytofix and Cytoperm kit. They were then incubated with rabbit anti-6xHis (5 μg/ml) followed by A647-conjugated goat anti-rabbit IgG. Flow cytometry acquisitions were done with a LSR Fortessa flow cytometer (Becton Dickinson) and results were analyzed using FlowJo 10.0.6 software.

2.10. Immunizations and sample collections

Five groups of 7 weaned pigs (28 days-old, 3 or 4 males and 3 or 4 females per group) were immunized as follows: intradermally with DNA on PLGA NPs (ID + NP), intradermally with naked DNA and surface electroporation (EP), intradermally with DNA on NPs and surface electroporation (EP + NP), with patches loaded with DNA and NPs (patch + NP), and with patches loaded with DNA and NPs and a final EP boost (patch + NP/EP). A group of 6 pigs were kept as controls. The electric pulses were set at 670 V/cm and the patches were applied on the lower thoracic area as described for pLuc above. For the ID + NP, EP and EP + NP, each PRRSV-AG encoding plasmid (320 μg) + pGM-CSF (80 μg) mixed in a final 400 μl volume of 0.9% NaCl was inoculated in 4 intradermal spots (100 μl each) under general anesthesia. Each pig of the ID + NP, EP, EP + NP and patch + NP group received 3 identical administrations, 4 weeks apart; the patch + NP/EP received 2 patch applications and a final EP boost, 4 weeks apart. Sera were harvested on D0, 35, 64, 84. Nasal swabs from the 2 nostrils were collected in PBS + anti-protease cocktail at D0 and 84. Spleen was harvested on D84 and spleen cells were collected as described [36]. At the end of the study, the animals were euthanized by an overdose of sodium pentothal.

2.11. Overlapping peptides

Overlapping peptides (20 mers, offset by 8 amino-acids) covering the NSP1β, RdRp, N and the GP4GP5M PRRSV antigens were synthetized by Mimotopes (Mimotopes Pty Ltd., Victoria, Australia, http://www.mimotopes.com). Upon receipt, the peptides were diluted in H_2O:acetonitrile (50:50 vol:vol) at a 5 mg/ml concentration and grouped as pools of peptides not exceeding 25 peptides: pool N (15 peptides), pool GP1 (from peptide1 to 20 of the GP4GP5M chimera), pool GP2 (from peptide 21 to 40 of the GP4GP5M chimera), pool NSP1β1 (from peptide 1 to 22), pool NSP1β2 (from peptide 23 to 47), pool RdRp1 (peptide 1 to 20), pool RdRp2 (peptide 21 to 40), pool RdRp3 (peptide 41 to 60), pool RdRp4 (peptide 61 to 80). A 20-mer peptide from the HIV polymerase was used as control.

2.12. Evaluation of PRRSV-AG-specific T cell responses by ELISPOT

IFNγ-secreting T cells were detected using PVDF membrane-bottomed 96-well plates (Multiscreen®$_{HTS}$, Millipore) coated with 15 μg/ml anti-porcine IFNγ (capture mAb) in PBS. Spleen cells were suspended in X-VIVO-20 medium supplemented with 2% FCS, 100 U/ml penicillin and 1 μg/ml streptomycin (culture medium) and 2×10^5 were plated per well. Cells were stimulated with the different pools of overlapping peptides described above at a 5 μg/ml final concentration for 18 h, in

duplicates. A HIV polymerase-derived peptide and ConA at 25 μg/ml were used as controls. Control wells with H_2O:acetonitrile were done. After 18 h, the IFNγ-secreting cells were revealed by sequential incubations with 0.5 μg/ml biotinylated anti-IFNγ followed by 0.5 μg/ml alkaline phosphatase conjugated-streptavidin and 1-Step™ BCIP/NBT reagent. The spots were enumerated using the iSPOT reader from Autoimmun Diagnostica GmbH. Positive wells were considered if the spot numbers in the 2 PRRSV stimulated conditions were strictly superior to the spot numbers in the control peptide stimulated conditions as described [37]. The mean number of spots of stimulated minus control peptide was calculated.

2.13. Evaluation of anti-N IgG and IgA by ELISA

The sera and swab extracts were assayed using the Ingezim PRRS 2.0 kit (Ingenasa, Spain) at a 1:40 and 1:2 dilution respectively. S/P ratio were calculated as follows: [OD sample minus OD negative control]:[OD positive control minus OD negative control]. For IgA, area flat bottom polystyrene high bind microplates (Corning) were coated overnight at 4 °C with 50 ng N recombinant protein (same preparation as in the Ingezim PRRSV 2.0 kit) in 50 μl of PBS. Plates were saturated with 0.1% skim milk in PBS - 0.05% Tween 20 for 2 h at 37 °C. Samples were 2-fold serially diluted and were incubated for 2 h at 20 °C. N antigen-bound IgA were detected using anti-pig IgA mAb (50 ng/ml) followed by HRP-conjugated rat anti-mouse IgG1 (500 ng/ml). All detection antibodies were incubated for 1 h at 37 °C. The 1-Step™ ULTRA-tetramethylbenzidine HRP substrate (TMB, Thermo-Scientific) was used and absorbance was measured at 405 nm.

2.14. Cytokine detection

Concentrations of IL-1β, IL-17 and IL-8 were assessed by cytometric beads assay for simultaneous detection of 12 swine cytokines (IL-4, IFNα, TNFα, IL-2, IL-8, IL-13, IL-12, IL-6, IFNγ, IL-10, IL-17, IL-1β) as described [38].

2.15. Statistical and correlation analysis

Data were analyzed with the GraphPad Prism 6.0 software. The unpaired non-parametric bilateral Mann-Whitney test was used to compare the efficacies of different V/cm and of delivery methods for induction of luciferase expression, the innate cytokine secretion and the IgG content in sera and swab extracts. The Wilcoxon signed rank test was used to compare the T cell response versus the non-vaccinated group.

3. Results

3.1. Formulating DNA plasmids with nanoparticles (NPs)

A previous work in the pig [39] identified that 400 μg DNA was an optimal DNA amount to immunize pigs, what we recently confirmed in sheep [37], therefore we selected this dose for all the delivery methods in this work. The coating of the DNA on cationic PLGA NPs aimed at promoting DNA stability in extracellular fluid and during the intracellular trafficking to the nucleus as well as at favoring the capture by skin cells including mononuclear phagocytes for antigen presentation [10,31]. Patch fabrication requires a concentrated formulation of 5.5 mg/ml DNA, associated with NPs, to be dispensed into a small volume of the microneedle mould. In initial testing, we determined that a 20:1 ratio of DNA:NPs was the best ratio for optimal loading of DNA on NPs without precipitation occurring. By measurement of free DNA (non-adsorbed to the NPs) in the formulation supernatant after centrifugation, we found that 15–20% of the total DNA was loaded on the NPs in this condition, in agreement with the high proportion of DNA vs NPs. The NPs coated with DNA at a 20:1 ratio measured between 120 and 140 nm and had a polydispersity index around 0.4. DNA adsorption onto the surface of the cationic NPs were also indicated by a drop of the zeta potential (from +15/+30 mV to −30/−50 mV).

3.2. Patches loaded with plain DNA or DNA combined to cationic PLGA NPs

We incorporated 44 μg of DNA plasmid per cm^2 patch, which is in the same order of magnitude as in previous studies where 50 μg DNA per cm^2 were used [19,22]. These patches contained 225 needles each (Fig. 1A), the needles were 500 μm high (Fig. 1B), and the total amount of DNA (plain DNA or associated to NPs at a 20:1 ratio) was 400 μg per 9 cm^2 patch. The quality of the patches was high, as reflected in the quality score reaching 100% (see Material and Methods). The patches were applied to the lower thoracic zone to permit a 20 N force to be applied for 1 min to the skin and as a convenient site for securely placing the patch and an Elastoplast wrap. This skin thickness in this zone is between 90 and 135 μm (not shown) and is therefore compatible with vaccine delivery through the epidermis with 500 μm-high needles. We previously characterised skin penetration events that occur in ex vivo pig skin with dissolvable microneedle patch administration, including with histological analyses [24,40].

3.3. Transduction efficacy of pig skin cells upon DNA delivery with patches, ID and surface EP

In order to evaluate the in vivo transfection efficacy of DNA plasmids delivery, we administered a plasmid encoding for a reporter luciferase gene (pLuc) using patches as well as the intradermal route (ID), or the ID route plus surface electroporation (EP), with plain DNA or DNA combined to cationic PLGA NPs. The optimal plasmid delivery V/cm parameter for EP had been established beforehand on test pigs, using escalating electric field values. A plateaued luciferase signal that did not induce local necrosis was obtained with the 670 V/cm parameter (Supplementary material 1) which was used for all the surface EP in this paper. A group of 3 pigs was used for ID administration in the ventral zone and EP in the inguinal zone (group 1), and another group of 3 pigs for patch administration in the lower thoracic zone and for EP in the inguinal zone (group 2) (Fig. 2A). A 100 μg DNA dose was chosen for EP and ID based on our previous successful gene transfer study in sheep skin using surface EP [37]. Skin biopsies were harvested after 24 h and processed for detection of luciferase expression by bioluminescence measurement. This timing was selected as shown to be optimal by others [41]. Control skin from the same thoracic (CtD for control patch), ventral (CtI for control ID) and inguinal zones (CtE for control EP) was collected, because different skin zones can differ in their intrinsic luminescence, in cell composition and in other biological properties. The level of bioluminescence induced by the ID route was significantly higher than the ventral control ($2.8 \times 10^6 \pm 2.63 \times 10^6$ vs. $5.62 \times 10^5 \pm 7.05 \times 10^5$ p/cm^2/s/r, $p < .05$), and the level induced by EP was clearly higher than the ID one's (group 1, $1.71 \times 10^8 \pm 1.87 \times 10^8$, $p < .01$) (Fig. 2B). The signal with patches loaded with plain DNA was also significantly higher than the thoracic control and reached $2.89 \times 10^7 \pm 1.88 \times 10^7$ p/cm^2/s/r in group 2, and EP delivery induced further higher levels, reaching $1.3 \times 10^8 \pm 1.46 \times 10^7$ p/cm^2/s/r in that group ($p < .01$, EP vs. patches). Coating NPs with DNA did not statistically change the level of bioluminescence in all 3 delivery methods (Fig. 2B). The comparison of transfection efficiency levels between ID and patches was not done from these results because ID and patch applications were not performed on the same pigs. In conclusion, skin cell transduction can be obtained with DNA-loaded patches as well as with ID delivery, although with lower efficacy than with EP, and the level of transduction does not significantly improve by loading the DNA on cationic PLGA NPs in our conditions.

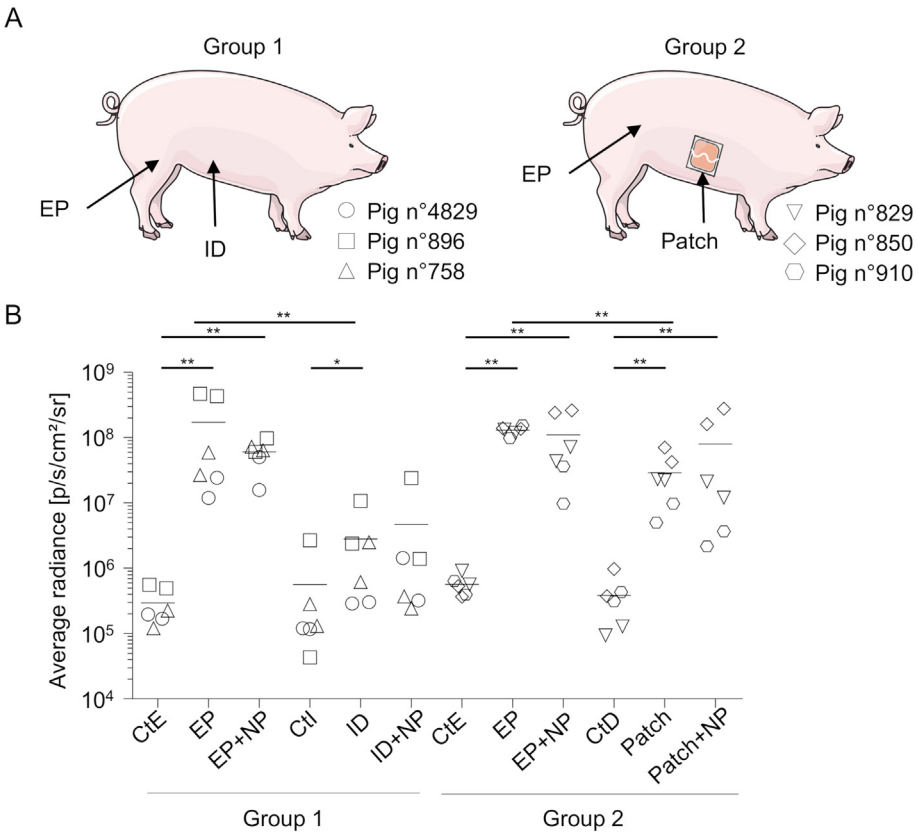


Fig. 2. Expression of luciferase activity upon in vivo transfection of pig skin cells with pLuc delivered using surface EP, ID and patch applications. (A). Large White pigs (Group 1: #4829, 896, 758 and Group 2: #829, 850 and 910) were anesthetized (see Material and methods). Group 1 received pLuc with EP and ID administration, Group 2 received pLuc with EP and patches. Each pig is represented by a distinct symbol (see legend on the figure). In the inguinal zone, 100 µg pLuc, either plain or adsorbed on cationic PLGA NP (20:1, DNA:NP ratio) was injected ID and the skin site was subjected to surface EP as described in the material and methods (EP and EP + NP). In the ventral zone, 100 µg pLuc, either plain or adsorbed on cationic PLGA NP was injected ID. In the thoracic area, patches loaded with pLuc plasmid (400 µg per 9 cm^2 patch), either plain or adsorbed on cationic PLGA NP (20:1, DNA:NP ratio) were applied on the skin as described in the material and methods (patch and patch + NP). (B). After 24 h, 8 mm biopsies were harvested at the sites of administration and processed for luciferase activity detection. Control skin of the same respective sites (CtE for EP control, CtI for ID control, and CtD for patch control) were collected and treated in parallel. The luciferase activity results (p/s/cm^2/sr) of the transfected and control skin from each pig are indicated by a distinct symbol and were obtained from independent duplicates. Significant differences between the injected sites and their respective control sites were determined with the non-parametric Mann-Whitney test (**, $p < .01$; *, $p < .05$). Similar results were obtained in an independent experiment.

3.4. Inflammatory cell mobilization induced by DNA delivery with patches and surface EP in skin

The immunogenicity of plasmid DNA vaccines has been shown to be associated both to cell transduction and to inflammatory cell mobilization, which has been proposed to have an adjuvant effect [15–17]. We therefore analyzed the mononuclear phagocyte and granulocyte cell types in skin biopsies 24 h after administration of plasmid with patches, ID or EP, with plain DNA or combined to cationic PLGA NPs. In order to relate these results to the immunogenicity experiment where pGM-CSF was used as a genetic adjuvant (see below), pLuc was combined to pGM-CSF (4:1, µg:µg ratio). The mononuclear cell subsets were identified based on our previous work on swine skin dendritic cells and macrophages [29,42] and on others [43]. The gating strategy is described in Supplementary material 2 on cells from control skin (A) and surface EP (B) biopsies. Granulocytes were identified as $6D10^{pos}$ cells. From our previous work [29,42], $CD172A^{pos}CD163^{high}$ were split in MHC class II^{pos} and ^{neg}, corresponding to $CD163^{high}$ dermal DCs (DDCs), homologous to human $CD14^{pos}$ DDCs, and $CD163^{high}$ macrophages (MPs) respectively. Among $CD163^{int/neg}$ MHC class II^{pos} cells, we distinguished $CD172A^{neg}CD13^{pos}$ cells which correspond to the conventional type 1 DC (cDC1) in human, mice and pigs [43–45]. These cells back-gate to MHC class II^{high} cells (supplementary material 2), as expected, both in the control and EP conditions [29,42]. Among $CD163^{int/neg}$ MHC class II^{pos} cells, we also distinguished $CD172A^{pos}CD163^{neg}$ and $CD172A^{pos}CD163^{int}$ cells. In the control condition, the $CD163^{int}$ cells back-gate mainly to MHC class II^{high} cells and the $CD163^{int}$MHC class II^{high} cells correspond to cDC2 DC, homologous to human CD1a dermal DC [29,42]. The $CD163^{neg}$ cells back-gate mainly to MHC class II^{high} cells and a large fraction of them express high levels of langerin (supplementary material 3) and correspond to Langerhans cells (LCs) [29,42]. However, upon EP, $CD163^{int}$ and ^{neg} cells expressed variable MHC class II among which the MHC class II^{high} cells cannot be distinguished. Furthermore, langerin expression is much reduced upon EP (supplementary material 3). Therefore, we will designate these 2 subsets as $CD163^{int}$ and $CD163^{neg}$ cells which are likely to correspond to heterogeneous populations of inflammatory monocytic cells mixed with cDC2 and LC respectively. Based on this gating, we analyzed the percentage of each subset among live cells (supplementary material 4) and the total live cells of each subset in a pool of 6 biopsies upon pLuc + pGM-CSF delivery, in 2 groups of pigs (Fig. 3A): group 1 (EP and ID) and group 3 (patch). The percentage of live cells were not significantly affected by EP (supplementary material 4) and the total live cell numbers in biopsy pools slightly varied between conditions, with the lower numbers found in the inguinal controls (Fig. 3B). Compared to control skin, ID and EP induced increased numbers of granulocytes, of MHC class II^{pos} $CD163^{int}$ and $CD163^{neg}$ cells, and EP had the strongest effects on these subsets recruitment, promoting also cDC1 accumulation (Fig. 3B). Cationic PLGA NPs combined to EP tended to enhance the recruitment of these different subsets, and especially of the MHC class II^{pos} $CD163^{int}$ and $CD163^{neg}$ cells (Fig. 3B). The increase in proportion (%) of these subsets' representation followed the same trend as their cell numbers in biopsy pools (supplementary material 4). Only the proportion of $CD163^{high}$ DDC and MP appeared to decrease with EP, suggesting that these later subsets are not or minimally recruited by EP (supplementary material 4). Conversely, patch application did not result in change in mononuclear phagocytes nor granulocytes representation (Fig. 3B, supplementary material 4). A histological examination was conducted 24 h after administration of DNA with patch and EP and confirmed the accumulation of inflammatory cells locally upon EP, both in the epidermis and dermis, whereas there was no detectable inflammation with patches (supplementary material 5). Altogether these results show that ID and EP induced the recruitment of inflammatory myeloid cell subsets whereas patches did not. EP + NP further enhanced inflammatory cell accumulation, especially of the MHC class II^{high} $CD163^{int}$ and $CD163^{neg}$ subsets.

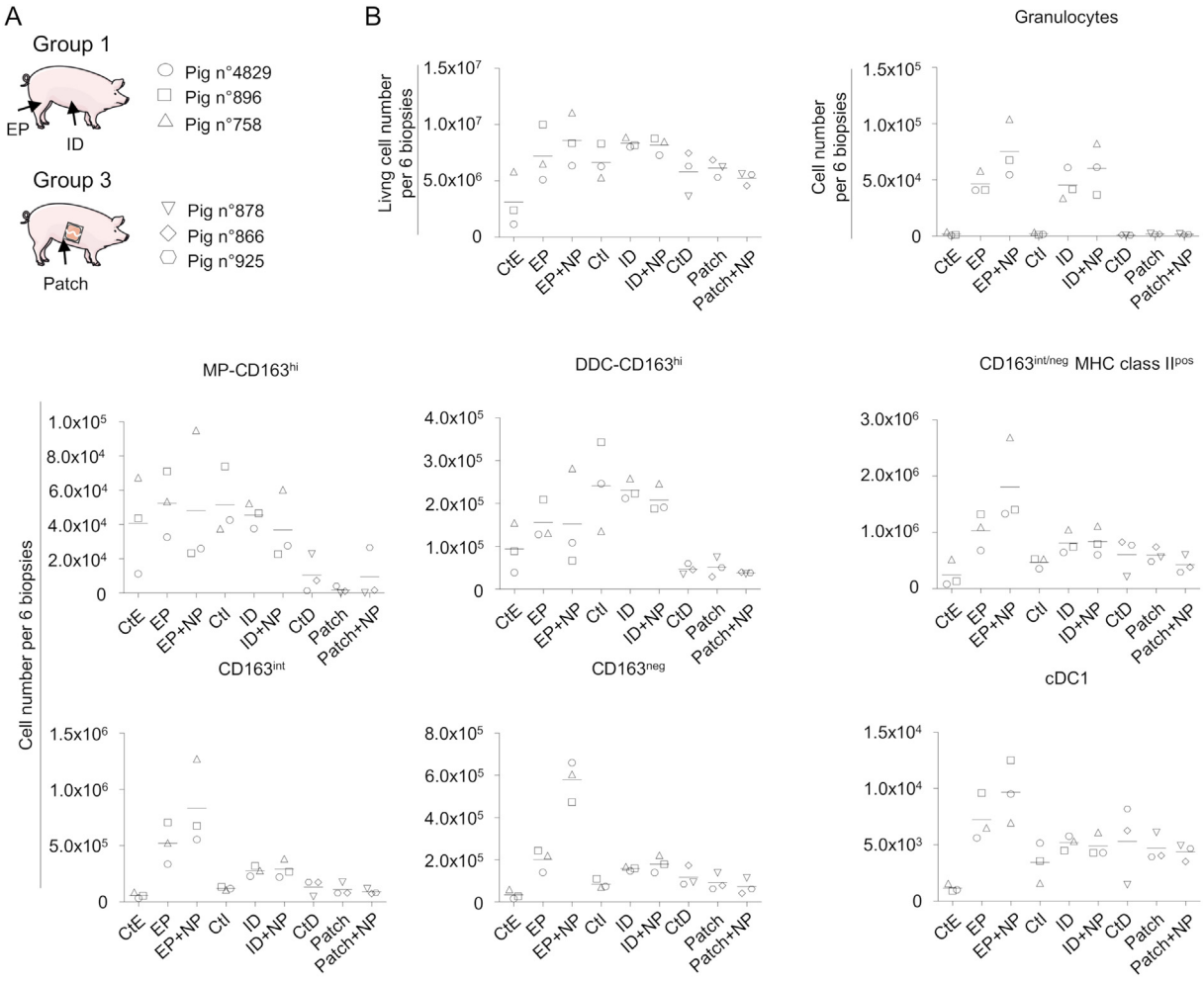


Fig. 3. Myeloid cell mobilization upon administration of pLuc and pGM-CSF delivered in skin using surface EP, ID and patch applications. **(A).** Large White pigs (Group 1: #4829, 896, 758 and Group 3: #878, 866 and 925) were anesthetized. Group 1 received pLuc + pGM-CSF with EP and ID administration, Group 3 received pLuc + pGM-CSF with patches. Each pig is represented by a distinct symbol (see legend on the figure). For this experiment, pGM-CSF was combined to pLuc (20 μg pGM-CSF + 80 μg pLuc in EP and 80 μg pGM-CSF + 320 μg pLuc in patches). **(B).** Six EP and ID sites were pooled per condition and 6 biopsies were pooled from patch sites and the biopsies were processed to skin cell dissociation as described in the material and methods. The total live cell number from the 6 biopsies, obtained with the Guava ViaCount assay, are reported. The total live cell numbers for each indicated subset in the 6 biopsies are shown. The delivery methods are named as in Fig. 2. The cell subset % among live cells are provided in supplementary material 4. No statistical test was conducted due to the < 5 values per condition; 6 biopsies were used to generate each value, with pairs between treatments and controls. Similar results were obtained in an independent experiment.

3.5. Inflammatory cytokine synthesis in skin upon DNA delivery with patches and surface EP

In order to further analyse the inflammation induced by the different DNA delivery methods, we harvested skin biopsies 24 h after pLuc +pGM-CSF administration and placed 2 biopsies per condition in flotation in 2 separate wells of culture medium for 24 h. The cytokine content was analyzed in a multiplex assay for the detection of 12 cytokines (IL-4, IFNα, TNFα, IL-2, IL-8, IL-13, IL-12, IL-6, IFNγ, IL-10, IL-17, IL1β). Surface EP, with or without cationic PLGA NPs, induced the secretion of IL-1β, IL-8, and IL17, but not of the other cytokines (Fig. 4). DNA delivered by patches did not induce detectable cytokine synthesis under these conditions (Fig. 4). Similar results were obtained when pLuc only (without GM-CSF) was used for the delivery with EP (supplementary material 6). Therefore, the delivery of DNA with patches allows gene transfer and expression in skin cells without detectable inflammatory response, whereas surface EP induces high reporter gene expression, inflammatory cell mobilization, and inflammatory cytokine expression.

3.6. Immune responses induced by DNA vaccine delivery with patches, ID and surface EP

The next step was to evaluate the immunogenicity induced by the DNA delivery with patches, ID and EP. We produced plasmids encoding for antigens from PRRSV, a swine arterivirus. Four antigens were selected based on their T and B cell antigenicity: N is the immunodominant B cell antigen, and GP4GP5M, RdRp and NSP1β include conserved T cell epitopes across distant viral strains [46,47]. The PRRSV antigens (PRRSV-AG) sequences were end-terminated by a 6xHis tag and cloned in a pcDNA3.1 expression vector. The 4 PRRSV-AG vectors were transiently transfected in 293 T cells and the 6xHis-tagged proteins were detected intracellularly by immunostaining and flow cytometry (Fig. 5A) and after cell lysis in RIPA buffer by Western Blot (Fig. 5B). Despite the known difficulty to detect 6xHis-tagged proteins due to histidine stretch content in cellular proteins, we could well detect the transfected PRRSV-AG, as compared to cells transfected with a control pcDNA3.1 vector (Fig. 5A and B). The 4 antigens were detected at expected MW sizes, although additional products were found possibly due to incomplete reduction or alternative codon usage, but in coding frame as 6xHis-tag terminated. These PRRSV-AG

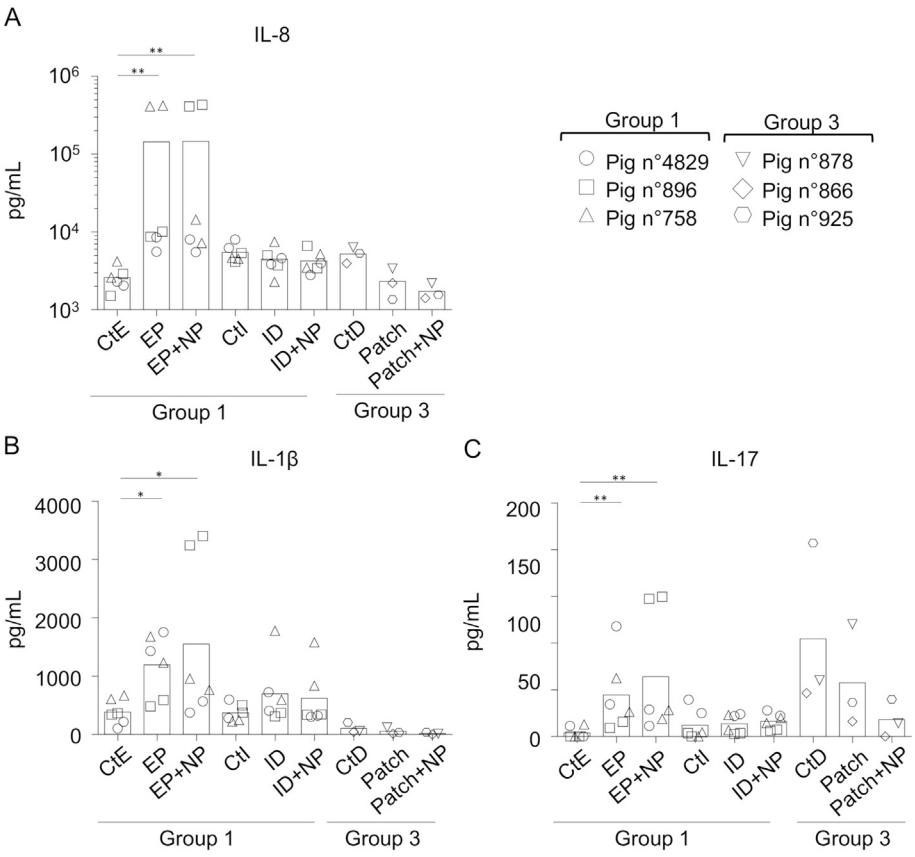


Fig. 4. Inflammatory cytokine secretion upon administration of pLuc and pGM-CSF delivered in skin using surface EP and patch application. The pLuc + pGM-CSF plasmids were administered by EP and ID injections in group 1 and by patches in group 3 as described in Fig. 3. Twenty-four hours after, skin biopsies from 2 same administration types were aseptically collected, washed in PBS and placed in 1 ml RPMI +10% FCS + 1% antibiotic/antimycotic cocktail for 24 h. Cytokines were detected using a multiplex cytometric bead assay and the cytokine concentration was evaluated using a standard curve with recombinant cytokines. The cytokine concentration of biopsies from each pig are indicated by a distinct symbol. Significant differences between the injected sites and control sites were determined with non-parametric Mann-Whitney test (**, $p < .01$; *, $p < .05$). **(A).** IL-8. **(B).** IL-1β. **(C).** IL-17. The bars represent the means.

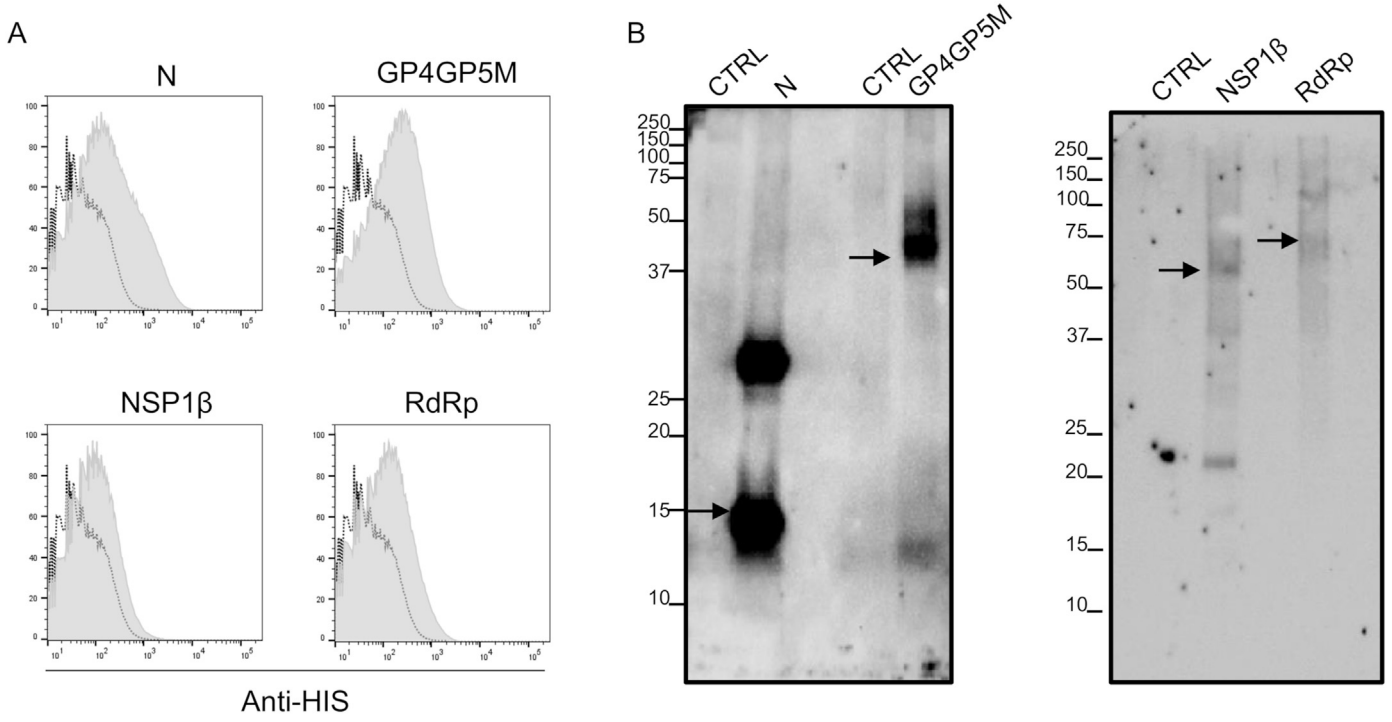
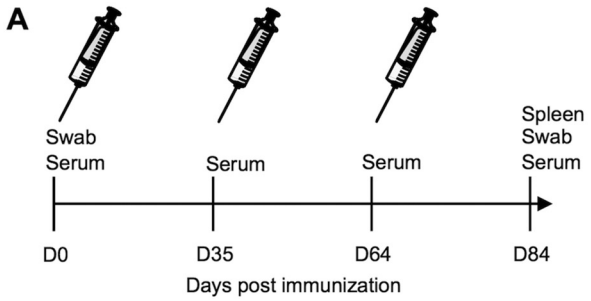


Fig. 5. PRRSV antigen expression in 293 T cells. 293 T cells were transfected with pcDNA3.1-ctrl or with pGP4GP5M, pN, pNSP1β, and pRdRp. After 2 days, cells were either processed to intracellular detection (A) or lysed in RIPA buffer (B). **(A).** PRRSV-AG terminated with 6xHis tag were detected, following 293 T cell permeabilization, with anti-6xHis rabbit polyclonal IgG followed by A647-conjugated goat anti-rabbit IgG. The 6xHis tag signal in each pPRRSV-AG transfected 293 T cells (grey background) is overlaid on the signal from pcDNA3.1-ctrl transfected 293 T cells and processed in parallel (dashed line). **(B).** A Western blot was done using anti-His rabbit IgG followed by HRP-conjugated anti-rabbit antibody. The samples (5 µg total protein) were migrated on the same SDS-PAGE gel under denaturing conditions. The bands at the expected theoretical molecular weight of each PRRSV protein are indicated with an arrow (N: 16 kDa, GP4GP5M: 37 kDa, NSP1b: 47 kDa and RdRp: 77 kDa). Note that no background is detected from the lane of 293 T cells transfected with pcDNA3.1-ctrl (CTRL lanes).



B

	None	EP	EP+NP	ID+NP	Patch+NP	Patch+NP/ EP
Pig number	6	7	7	7	7	7
D0	-	EP	EP+NP	ID+NP	Patch+NP	Patch+NP
D35	-	EP	EP+NP	ID+NP	Patch+NP	Patch+NP
D64	-	EP	EP+NP	ID+NP	Patch+NP	EP

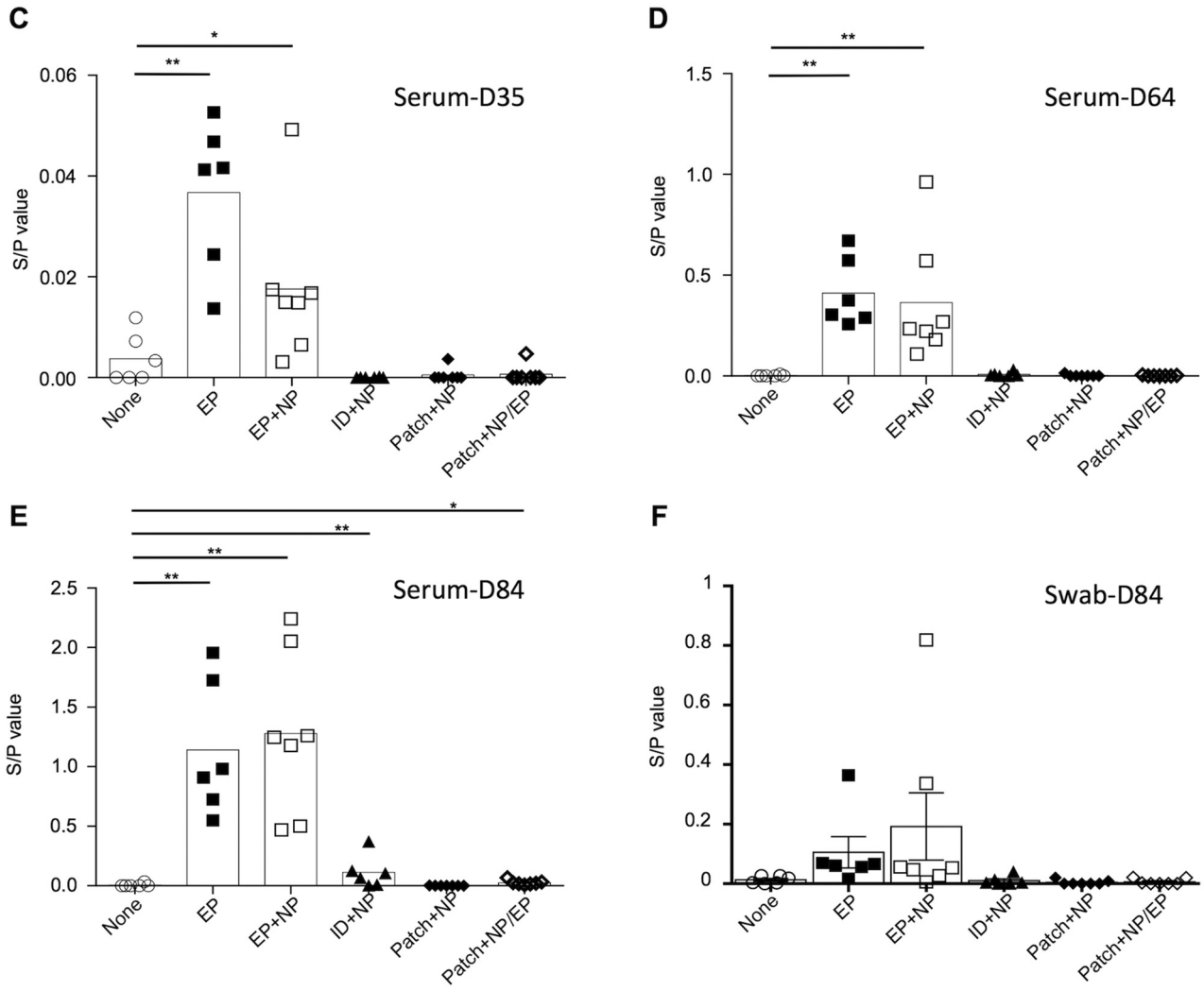


Fig. 6. Detection of IgG in sera and nasal secretions from pigs immunized with pPRRSV-AG delivered using surface EP, ID and patches. **(A and B).** Schematic representation of the immunization protocol of pigs with pPRRSV-AG + pGM-CSF. **(A)** Each pig received 320 μg of each pPRRSV-AG combined to 80 μg pGM-CS on day (D)0, D35 and D64 (see material and methods and B). Sera were collected at D0, D35, D64, D84, nasal swab at D0 and D84 and spleen cells were collected at D84. **(B).** Table is summarizing the 6 different vaccinated groups. Intradermal inoculations of plasmid coated on cationic PLGA NPs (ID + NP group), intradermal inoculations of plain DNA followed by EP (EP group), intradermal inoculations of plasmid coated on cationic PLGA NPs followed by EP (EP + NP group), or plasmid on NPs delivered by patch applications (patch + NP group) were performed on D0, D35 and D64. In the case of the patch + NP/EP group, plasmid DNA was delivered with patch + NP on D0 and D35 and with intradermal inoculation + EP on D63. **(C-E).** The sera (1:40) from D35 (C), D64 (D) and D84 (E) were assayed for detection of anti-N IgG using the Ingezim PRRS 2.0 kit. S/P ratios were calculated as described in the Material and Methods. **(F).** Nasal swab extracts (1:2) were assayed for detection of anti-N IgG using the Ingezim PRRS 2.0 kit on D84. Significant differences between the vaccinated groups and the control group were determined with the non-parametric Mann Whitney test (* $p < .05$, **, $p < .01$).

encoding vectors were therefore suitable to provide PRRSV B and T cell epitopes. Pigs were then immunized with 320 μg of these vectors, each combined with 80 μg pGM-CSF in 5 vaccinated groups and one non-vaccinated control group. The vaccinated groups (7 pigs in vaccinated groups initially, 6 in the control group) included: a group receiving DNA with cationic PLGA NP directly injected in the dermis (ID + NP), 2 groups receiving plasmids intradermally followed by surface EP with naked DNA (EP) and DNA adsorbed on cationic NPs (EP + NP), a group receiving DNA delivered by patches with cationic PLGA NPs (patch + NP), and finally a group primed twice with patches (DNA with NPs) and finally boosted with naked DNA and EP (patch + NP/EP) (Fig. 6A-B). There was one dead pig in the EP and ID + NP groups, due to

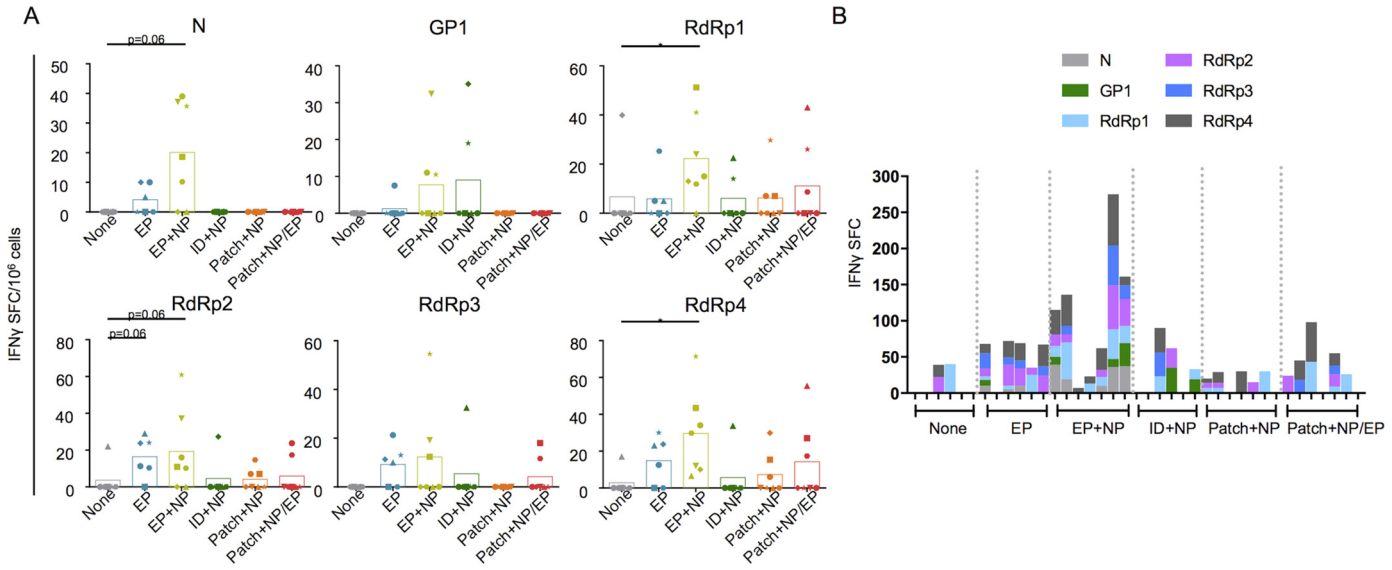


Fig. 7. Detection of IFNγ-secreting cells in spleen from pigs immunized with pPRRSV-AG delivered using surface EP, ID and patches. Splenocytes (2.5×10^5) were plated in Multiscreen plates coated with a capture anti-porcine IFNγ mAb (duplicated wells) and re-stimulated for 18 h with 5 μg/ml of peptide pools made of < 25 overlapping peptides covering the N, pool GP1 (from peptide 1 to 20 of the GP4GP5M chimera), pool RdRp1 (peptide 1 to 20), pool RdRp2 (peptide 21 to 40), pool RdRp3 (peptide 41 to 60), pool RdRp4 (peptide 61 to 80). An irrelevant peptide (5 μg/ml) or plain medium were used as controls. IFNγ spot forming cell (SFC) counts were considered PRRSV-AG-specific when both duplicated well values from cells stimulated with PRRSV peptides were strictly superior to the duplicated-well values from cells stimulated with the irrelevant peptide. **(A)** The mean SFC number in stimulated wells minus the ones with irrelevant peptide wells are shown per pig for each peptide pool (net mean values). Each symbol in the graphs represents an individual animal and the same symbol is used across the peptide pool restimulation. The box plot is drawn on the mean values obtained with the different pigs. Significant differences between the vaccinated groups and the control group were determined with the non-parametric Wilcoxon test (*, $p < .05$). **(B)** The net IFNγ SFC numbers upon stimulation is compiled for all peptides in each sheep, showing the breadth and the magnitude of the response.

anesthesia. The anti-N IgG levels were assayed from sera and nasal swab extracts using a commercial kit. Anti-N IgG were detectable at 35 and their levels further increased at D64 and D84, both in the EP and the EP + NP groups, and not in the patch groups (Fig. 6C-E). Low but significant anti-N IgG amounts were detected at D84 in ID + NP groups (Fig. 6E). No effect of DNA adsorption on cationic NP was observed on the anti-N IgG response in the EP conditions (Fig. 6C-E). Low levels of anti-N IgG were detected in nasal swab extracts in the EP and EP + NP group (Fig. 6F). Anti-N IgA could not be detected at D84, neither in sera nor in swab extracts.

The splenocytes were re-stimulated with overlapping peptide pools from the PRRSV-AG and the IFNγ-secreting cells were detected (Fig. 7A, Table 1). Nine pools of maximum 25 peptides were used in order to stimulate splenocytes with 1 μg of each peptide per well without toxicity (see Material and Methods). Non-specific responses in control pigs were obtained with the GP2 and NSP1β pools, possibly due to cross reactivity of the TCR with unrelated T cell epitopes to which these pigs have been exposed, therefore these pools were not considered in the analysis. No antigen was highly dominant compared to the other antigens; each animal demonstrated a *unique* hierarchy of antigen recognition, irrespective of vaccine. However, N, RdRp1 and RdRp4 induced the most consistent responses across pigs and vaccine regimens. A Wilcoxon signed rank test reveals statistically significant differences between the response magnitudes in the EP + NP and the control group in the case of the RdRp1 and RdRp4 pools, and close to significance with the N and RdRp2 pool (Fig. 7A). Fig. 7B shows a stack bar plot of the responses to peptide pools per pig and illustrates that the breadth and magnitudes of the IFNγ responses are higher in the EP + NP groups vs the other groups. For each pig, the number of peptide pools able to stimulate splenocytes was calculated and the proportion of pigs capable to respond to > 2 peptide pools was 0/6 in the control group, 1/6 in the ID + NP, 1/7 in the patch + NP/EP group, 2/7 in the patch + NP group, 4/6 in the EP group and 5/7 in the EP + NP group (Table 1). Altogether this immunogenicity analysis shows that DNA delivery with patches induced no significant B and T cell responses, DNA delivery with ID induced low but significant B cell responses, whereas delivery with EP induced substantial IgG responses in all pigs and DNA adsorption on cationic PLGA NPs combined to EP promoted the magnitude and breadth of the IFNγ T cell responses.

4. Discussion

DNA delivery with dissolvable microneedle patches is an emerging technology with advantages such as elimination of needles and hazardous waste, improved vaccine thermo-stability, potential dose-sparing capacity and self-administration. However, it was unknown if the potency of a DNA vaccine can be enhanced by patch delivery into the skin in a relevant preclinical model such as pigs. In this work, we evaluated DNA delivery by patches compared to simple ID and EP in the pig via skin. We found that, although plasmid DNA was expressed in skin upon patch application, no significant T and B cell responses were induced to the PRRSV-AGs, whereas simple ID induced mild but significant B cell responses and EP induced higher IgG and IFNγ-T cell responses, especially when DNA was combined to cationic PLGA NPs. We also found that patches, with DNA combined or not on cationic PLGA NPs, did not induce detectable local innate response whereas simple ID and especially EP did induce substantial local inflammatory responses. These results show that the combination of transfection efficiency with local innate immune responses (myeloid cell recruitment and cytokine expression) is associated with immunity induced by DNA delivery methods. This finding suggests avenues for improving the immunogenicity of patches by addition of innate immunity stimulants in pigs and likely in humans.

The pig is considered as the preclinical model of choice by the scientific community and health authorities to evaluate the efficacy and toxicity of drug delivery through skin as well as to study wound healing mechanisms [48]. Anatomical, physiological and immunological properties of pig skin also support the pertinence of this animal model for assessing needle-free vaccine delivery [49]. Indeed, pig and human skin share the same general structure, thickness, hair follicle content,

Table 1
IFNγ-secreting T cells in the pPRRSV-AG vaccinated groups upon re-stimulation with overlapping peptide pools (N, GP1, RdRp1, RdRp2, RdRp3, RdRp4).

Vaccine	Pig N°	Peptide pools						Nb of stimulating peptide pools/pig	% responding pigs to > 2 peptides/group
		N	GP1	RdRp1	RdRp2	RdRp3	RdRp4		
None	6	0	0	0	0	0	0	0	0/6
	44	0	0	0	0	0	0	0	
	48	0	0	0	22	0	17	2	
	55	0	0	40	0	0	0	1	
	57	0	0	0	0	0	0	0	
	78	0	0	0	0	0	0	0	
EP	13	10	8	5	11	21	13	6	4/6
	17	0	0	0	0	0	0	0	
	38	5	0	5	29	10	23	5	
	39	10	0	0	24	11	24	4	
	67	0	0	25	10	0	0	2	
	68	0	0	0	24	13	30	3	
EP + NP	7	39	11	15	16	0	34	5	5/7
	37	19	0	51	11	12	43	5	
	46	0	0	0	0	0	7	1	
	47	0	0	13	0	0	10	2	
	59	10	0	12	10	0	30	4	
	72	36	11	41	61	55	71	6	
	76	37	32	24	37	19	12	6	
ID + NP	10	0	0	0	0	0	0	0	1/6
	36	0	0	0	0	0	0	0	
	45	0	0	23	0	33	34	3	
	71	0	35	0	27	0	0	2	
	75	0	0	0	0	0	0	0	
	77	0	19	14	0	0	0	2	
Patch + NP	2	0	0	7	7	0	6	3	2/7
	12	0	0	7	7	0	15	3	
	16	0	0	0	0	0	0	0	
	25	0	0	0	0	0	30	1	
	35	0	0	0	15	0	0	1	
	53	0	0	30	0	0	0	1	
	58	0	0	0	0	0	0	0	
Patch + NP/EP	11	0	0	0	24	0	0	1	1/7
	14	0	0	0	0	18	27	2	
	23	0	0	43	0	0	55	2	
	54	0	0	0	0	0	0	0	
	56	0	0	9	17	12	17	4	
	65	0	0	26	0	0	0	1	
	74	0	0	0	0	0	0	0	

pigmentation, collagen and lipid composition, by opposition with rodents [50]. In addition, the immune and inflammatory responses of human and pigs are closer to each other than to the rodent ones [51]. Furthermore, the immune and inflammation-related gene families expanded or contracted with similar rates during human and pig evolution but with much higher rates than in rodents, and the structural functional protein-domain of orthologous immune and inflammation-related genes show a higher degree of preservation between human and pig than between these species and rodents [52] [53]. This convergent genetic evolution might be related to shared selection pressures by the same families of pathogens such as intestinal worms and by zoonotic agents such as influenza, rotavirus, *Campylobacter*, *Toxoplasma gondii* etc. [54]. Correlatively pig and human macrophages present similar genomic responses during M1 polarization upon LPS stimulation, whereas mouse macrophage genomic response appears more distant [52,55,56]. Our group also showed that pig and human skin display similar subsets of dendritic cells and macrophages in the epidermis and dermis, based on comparative transcriptomes and functional analyses [29]. Therefore, pig presents skin tissue and immune characteristics more relevant than the rodent ones for prediction of efficacy of needle-free delivery of vaccines such as DNA vaccines with patches in human.

Significant transduction of skin cells in pigs was obtained with patches as previously published in mice with DNA and viral vectors [21,26,40]. However, in contrast with other studies using solid microneedle in mice [31,57], we did not measure a benefit of DNA combination to cationic PLGA NPs in terms of transgene expression at 24 h. This may highlight difference in potency of DNA vaccines in mice compared to larger animals. This difference may also be due to using net negatively charged DNA-conjugated particles, whereas net positively charged plasmid DNA-cationic NP complexes were shown to be the most favorable to immunogenicity [31]. In addition, as explained in the result section, only about 15–20% of DNA is adsorbed on cationic PLGA NPs, therefore most of the DNA is naked in our formulations and this excess of free DNA may explain the lack of detectable benefit of NPs in transgene expression. It is also possible that the NP benefit would be obtained at a later time point than 24 h, considering the expected increase in stability of DNA associated to NPs. The DNA load in patches is 44 μg/cm^2 patch, therefore a skin biopsy (0.5 cm^2) corresponds to a theoretical delivery of 22 μg DNA whereas in the case of EP, the biopsy roughly corresponds to the whole delivery of 100 μg DNA. Therefore, it is possible that the efficiency of gene transfer by patch per μg DNA is pretty high, although escalating doses should be used with both delivery methods in order to make a conclusive statement. It is also possible that the transfected cell types in skin are different between the different methods. In the case of surface EP, the dominant transduced cell types vary between studies, and were identified as keratinocytes, fibrocytes, dendritic-like cells, adipocytes or myocytes, possibly due to differences in the investigated species and in the precise site of injection in the dermis [17,58,59]. The transduced cells have not yet been identified in the case of dissolvable microneedle patches, to the best of our knowledge. Cell localization studies involving refined imaging technologies such as cleared in-toto tissue and confocal microscopy

with suitable reagents will be needed to reliably assess the in vivo transfected cell type and their location in the skin or elsewhere [60]. It is also possible that DNA combination with PLGA NPs alters the cell type that capture the DNA, and favors cells endowed with higher macropinocytosis capacities, especially after the EP pulses.

Efficient immunogenicity of DNA vaccination has been previously related to inflammatory cell mobilization induced by the delivery method [16,17]. In monkey, surface EP was shown to induce the accumulation of granulocytes and of MHC class II^{pos} antigen-presenting cells expressing variable levels of CD163 [17]. In our pig experiment, we confirm the strong accumulation of granulocytes upon surface EP and of different types of MHC class II^{pos} cells, i.e. cDC1, $CD163^{neg}$ and $CD163^{int}$ subsets (Fig. 3). As explained in the results, the exact identity of the last two subsets could not be determined and they probably correspond to heterogeneous populations of inflammatory $CD172A^{pos}$ monocytic cells and LC ($CD163^{neg}$) and cDC2 ($CD163^{int}$). The precise assignment of MHC class II^{pos} $CD172A^{pos}$ cells to a defined subset under inflammatory conditions cannot be done currently with multi-parameter flow cytometry, not only in pigs, but also in the reference mouse and human species [61]. Such an assignment requires sophisticated analyses, such as comparative transcriptome at the single cell level, due to still blurry phenotypes of MHC class II^{pos} $CD172A^{pos}$ subsets [62–64]. Of note, NPs added to EP tended to further enhance the recruitment of inflammatory cells and especially of the MHC class II^{pos} $CD163^{int}$ and $CD163^{neg}$ subsets. Further insight in the composition of these cell populations would be of interest to understand the adjuvant effect of NPs in our setting.

Together with the inflammatory cell mobilization, we found that EP, with and without PLGA NPs, induced the synthesis of IL-8, IL-17 and IL-1β. IL-8 and IL-17 are involved in immune cell recruitment and IL-1β is recognized as an important cytokine that is released in response to cellular stress and damage associated molecular patterns and which effectively activates antigen presenting cells and adaptive immunity [65]. Patches, with and without NP, did not induce detectable inflammatory cell mobilization nor inflammatory cytokine secretion. We also previously demonstrated significantly reduced cytokine induction when vaccines were administered to mice using silicon microneedle arrays compared to ID delivery [66,67]. Our findings support the hypothesis that patch delivery in pigs does not cause the innate activation necessary for immunogenicity; this is in contrast to EP or even simple ID. Therefore, inclusion of an inflammatory adjuvant could be beneficial to patch immunogenicity, such as shown in pigs in the case of the skin administration of protein hepatitis B surface antigen (HBsAg) coated onto polyanhydride poly(bis(p-carboxy-phenoxy)propane microneedle [49] or in dissolvable microneedle patches with QS-21 [68]. In the latter case, HBsAg-specific antibody responses were not induced in the absence of adjuvant. Alternatively, non-ablative fractional laser treatment [69] may also enhance DNA patch immunogenicity. Spring-loaded applicators have been tested in human with coated microneedle arrays and it has been suggested that these induced a necrotic-based inflammatory reaction which adjuvants the immune response to antigen [70]. TLR4 and 9 ligands were previously shown in mice to synergize with DNA vaccination [12]. A TLR7 ligand, which induces a strong skin inflammation [71], may be particularly suitable in the case of DNA-loaded patches. Further work is required to identify an adjuvant that induces strong vaccine-induced immunity while minimizing skin reactions and to understand which innate cell populations are required for this response.

pPRRSV-AG DNA combined to cationic PLGA NPs and loaded on patches did not induce significant IFNγ T-cell responses nor IgG responses. It should be emphasized that PRRSV-AG are intrinsically weak antigens [72], and this property may have affected the immunogenicity results that we obtained in our side-by-side assessment of DNA delivery methods. Indeed, as a matter of comparison with other DNA vaccines delivered by simple ID in pigs, antibody responses against pseudorabies [73,74] or foot and mouth disease viruses [75] [76] were detected after one or two DNA vaccine injections, which is not the case with our PRRSV DNA vaccine, for which 3 injections were needed to detect anti-N IgG with the very sensitive commercial ELISA. Notably, despite the low intrinsic immunogenicity of PRRSV-AGs, we found that EP delivery induced substantial IgG responses and IFNγ T-cell responses, especially when the DNA was combined to cationic PLGA NP, a regimen which increased the breadth of the T-cell response. We did not observe an effect of cationic PLGA NPs on skin cell transduction nor cytokine production at 24 h, but some effect on myeloid cell recruitment, notably of the MHC class II^{pos} $CD163^{int}$ and $CD163^{neg}$ cells. The positive effect of cationic PLGA NPs versus plain EP on the IFNγ T-cell response may be related to this myeloid cell recruitment, to an improved DNA sensing during DNA uptake, or to changes in the transduced cell type. Notably, the magnitude of the B and T-cell responses that was achieved with EP + NP are in the same order as the one reported after immunization with attenuated PRRSV vaccines in previous reports [47,77,78]. Therefore our EP + NP regimen is a promising delivery strategy, especially in the perspective of a vaccine development relying on broad T-cell responses. It may also be advantageously used as a priming vaccine with an attenuated PRRSV vaccine boost, in order to optimize the T-cell response breadth and develop effective control strategies of this damaging infection in the pig industry.

The framework of our study in pig, that includes antigen expression and innate and adaptive immunity assessments, could be adapted to the other type of nucleic acid-based vaccine, the RNA vaccine, which holds high promises in vaccinology. The fragility of RNA has been the major hurdle against the wide development of RNA vaccines but recent methods have considerably improved RNA stabilization and reduced adverse reactive responses [1,2]. RNA vaccines share many properties with DNA vaccines but they have potential advantages over DNA vaccines regarding safety (no risk of integration in the genome), easier production (no high scale fermentation), and immunogenicity [79,80]. For the moment, the higher number of conducted clinical trials with DNA versus RNA vaccines [3] and the authorization for use in veterinary medicine [9,10] together with the current higher stability outside cold chain, continue to give support to the DNA vaccines, but RNA vaccines may reveal to be more immunogenic and possibly cost-effective in the long run [79,80]. As RNA and DNA vaccines differ in the number of membranes to be crossed for expression, and in the sensing pathways for triggering innate immunity [2], optimal delivery methods may differ. As RNA vaccines appear to be well delivered with liposome-based technology [79,80] and are intrinsically highly immuno-stimulatory [81], their delivery with patches may lead to better immunogenicity results than that of DNA, and should be evaluated in the near future.

5. Conclusion

Altogether, our study shows that surface electroporation with cationic NP is the most efficient DNA delivery method to elicit T and B cell responses in pigs. New portable systems using the EP principle suggest that this technology has a practical clinical future both in human and possibly in veterinary medicine [59]. Although dissolvable microneedle patches were efficient at delivering DNA vaccines and resulted in good transgene expression in skin, patch-based delivery did not induce inflammatory signaling and detectable immunogenicity and could be improved with adjuvants for eliciting the desired adaptive immune response in the pig and likely in human.

Declaration of competing interests

Anne Moore is an inventor of patents that have been or may be licensed to companies developing microneedle-based products. This potential competing interest has been disclosed and is being managed by University College Cork.

Dennis McDaid is Chief Operating Officer and current director and

owns stock in Xeolas Pharmaceuticals Limited. JMcC, DC and AD are former employees of Xeolas Pharmaceuticals Limited and have no financial or other competing interests. The other authors have no competing interest to declare.

Acknowledgements

We are grateful to Frédéric Martinon (CEA, Fontenay, France) for his guidance and lending of the CUY 21 Edit System apparatus. We thank François Lefèvre (INRA, Jouy-en-Josas, France) for the pGM-CSF plasmid, Bernard Delmas for the anti-CD13 mAb, and Stéphane Biacchesi (INRA, Jouy-en-Josas, France) for the pLuc plasmid. We are grateful to Mohammed Moudjou for his advices on the Western Blot technique. We thank the DIM-ASTREA and the Department of Animal Health at INRA for the financial support allowing the purchase of the ispot/fluorospot. We thank Conor O'Mahony for the microneedle moulds (Tyndall National Institute, Cork). We thank the MIMA2 Microscopy and Imaging Regional Strategic Platform for the access to IVIS-200 (INRA OC N°35 CNOC) and the Investissement d'Avenir (ANR-11-INBS-008). This work has benefited from the facilities and expertise of @BRIDGe (GABI, INRA-AgroParisTech, Paris-Saclay University, France). This project has received funding from the European Union's Horizon 2020 Programme for research, technological development and demonstration under the Grant Agreement n633184. This publication reflects the views only of the author, and not the European Commission (EC). The EC is not liable for any use that may be made of the information contained herein.

Author contributions

CB-C: performed most of the experiments, analyzed results and draw the figs.

CU: performed experiments (immunizations, ELISA, cell mobilization analyses, plasmid preparation).

JMcC, DC, AD, DMcD: produced the patches and performed their quality check.

VJ, CB-Q, NC: produced the cationic NPs and performed their quality check.

Edwige B, Elise B, CB, OB, J-JL: performed and organized the animal experiments.

FB: optimized and performed the cytokine dosages

VC: assisted in the ELISPOT analyses

NB: participated to the design, to the analyses (cell mobilization analyses), to the animal experiments, to editing the manuscript.

AM: designed the study, directed the patches' preparation, analyzed results, edited the manuscript.

IS-C: designed and directed the study, coordinated the financial support and the experiments, wrote the request to the ethic committees, performed experiments, guided the analyses of the results, wrote the initial draft of the manuscript.

Appendix A. Supplementary data

Supplementary data to this article can be found online at https://doi.org/10.1016/j.jconrel.2019.06.041.

References

[1] N. Pardi, M.J. Hogan, F.W. Porter, D. Weissman, mRNA vaccines - a new era in vaccinology, Nat. Rev. Drug Discov. 17 (2018) 261–279.
[2] S. Rauch, E. Jasny, K.E. Schmidt, B. Petsch, New vaccine technologies to combat outbreak situations, Front. Immunol. 9 (2018) 1963.
[3] J.J. Suschak, J.A. Williams, C.S. Schmaljohn, Advancements in DNA vaccine vectors, non-mechanical delivery methods, and molecular adjuvants to increase immunogenicity, Hum Vaccin Immunother 13 (2017) 2837–2848.
[4] D. Hobernik, M. Bros, DNA vaccines-How far from clinical use? Int. J. Mol. Sci. 19 (2018).
[5] T.J. Kim, H.T. Jin, S.Y. Hur, H.G. Yang, Y.B. Seo, S.R. Hong, C.W. Lee, S. Kim, J.W. Woo, K.S. Park, Y.Y. Hwang, J. Park, I.H. Lee, K.T. Lim, K.H. Lee, M.S. Jeong, C.D. Surh, Y.S. Suh, J.S. Park, Y.C. Sung, Clearance of persistent HPV infection and cervical lesion by therapeutic DNA vaccine in CIN3 patients, Nat. Commun. 5 (2014) 5317.
[6] M.T. van Diepen, R. Chapman, N. Douglass, S. Galant, P.L. Moore, E. Margolin, P. Ximba, L. Morris, E.P. Rybicki, A.L. Williamson, Prime boost immunisations with DNA, MVA and protein-based vaccines elicit robust HIV-1, Tier 2 neutralizing antibodies against the CAP256 superinfecting virus, J. Virol. 93 (2019).
[7] P. Tebas, C.C. Roberts, K. Muthumani, E.L. Reuschel, S.B. Kudchodkar, F.I. Zaidi, S. White, A.S. Khan, T. Racine, H. Choi, J. Boyer, Y.K. Park, S. Trottier, C. Remigio, D. Krieger, S.E. Spruill, M. Bagarazzi, G.P. Kobinger, D.B. Weiner, J.N. Maslow, Safety and immunogenicity of an anti-Zika virus DNA vaccine - preliminary report, N. Engl. J. Med. (2017), https://doi.org/10.1056/NEJMoa1708120.
[8] C.L. Trimble, M.P. Morrow, K.A. Kraynyak, X. Shen, M. Dallas, J. Yan, L. Edwards, R.L. Parker, L. Denny, M. Giffear, A.S. Brown, K. Marcozzi-Pierce, D. Shah, A.M. Slager, A.J. Sylvester, A. Khan, K.E. Broderick, R.J. Juba, T.A. Herring, J. Boyer, J. Lee, N.Y. Sardesai, D.B. Weiner, M.L. Bagarazzi, Safety, efficacy, and immunogenicity of VGX-3100, a therapeutic synthetic DNA vaccine targeting human papillomavirus 16 and 18 E6 and E7 proteins for cervical intraepithelial neoplasia 2/3: a randomised, double-blind, placebo-controlled phase 2b trial, Lancet 386 (2015) 2078–2088.
[9] C. Collins, N. Lorenzen, B. Collet, DNA vaccination for finfish aquaculture, Fish Shellfish Immunol. 85 (2018) 106–125.
[10] J.S. Tregoning, E. Kinnear, Using plasmids as DNA vaccines for infectious diseases, Microbiol Spectr 2 (2014).
[11] J. Lloyd, J. Cheyne, The origins of the vaccine cold chain and a glimpse of the future, Vaccine 35 (2017) 2115–2120.
[12] F. Saade, N. Petrovsky, Technologies for enhanced efficacy of DNA vaccines, Expert Rev Vaccines 11 (2012) 189–209.
[13] A. Gothelf, J. Gehl, What you always needed to know about electroporation based DNA vaccines, Hum Vaccin Immunother 8 (2012) 1694–1702.
[14] K. Schultheis, T.R.F. Smith, W.B. Kiosses, K.A. Kraynyak, A. Wong, J. Oh, K.E. Broderick, Delineating the cell death mechanisms associated with skin electroporation, Hum Gene Ther Methods 29 (2018) 177–188.
[15] C.Y. Calvet, F.M. Andre, L.M. Mir, Dual therapeutic benefit of electroporation-mediated DNA vaccination in vivo: enhanced gene transfer and adjuvant activity, Oncoimmunology 3 (2014) e28540.
[16] S. Babiuk, M.E. Baca-Estrada, M. Foldvari, D.M. Middleton, D. Rabussay, G. Widera, L.A. Babiuk, Increased gene expression and inflammatory cell infiltration caused by electroporation are both important for improving the efficacy of DNA vaccines, J. Biotechnol. 110 (2004) 1–10.
[17] B. Todorova, L. Adam, S. Culina, R. Boisgard, F. Martinon, A. Cosma, M. Ustav, T. Kortulewski, R. Le Grand, C. Chapon, Electroporation as a vaccine delivery system and a natural adjuvant to intradermal administration of plasmid DNA in macaques, Sci. Rep. 7 (2017) 4122.
[18] J.A. Mikszta, J.B. Alarcon, J.M. Brittingham, D.E. Sutter, R.J. Pettis, N.G. Harvey, Improved genetic immunization via micromechanical disruption of skin-barrier function and targeted epidermal delivery, Nat. Med. 8 (2002) 415–419.
[19] H.S. Gill, J. Soderholm, M.R. Prausnitz, M. Sallberg, Cutaneous vaccination using microneedles coated with hepatitis C DNA vaccine, Gene Ther. 17 (2010) 811–814.
[20] S. Marshall, L.J. Sahm, A.C. Moore, The success of microneedle-mediated vaccine delivery into skin, Hum Vaccin Immunother 12 (2016) 2975–2983.
[21] G. Cole, A.A. Ali, C.M. McCrudden, J.W. McBride, J. McCaffrey, T. Robson, V.L. Kett, N.J. Dunne, R.F. Donnelly, H.O. McCarthy, DNA vaccination for cervical cancer: strategic optimisation of RALA mediated gene delivery from a biodegradable microneedle system, Eur. J. Pharm. Biopharm. 127 (2018) 288–297.
[22] J.M. Arya, K. Dewitt, M. Scott-Garrard, Y.W. Chiang, M.R. Prausnitz, Rabies vaccination in dogs using a dissolving microneedle patch, J. Control. Release 239 (2016) 19–26.
[23] Y. Ma, W. Tao, S.J. Krebs, W.F. Sutton, N.L. Haigwood, H.S. Gill, Vaccine delivery to the oral cavity using coated microneedles induces systemic and mucosal immunity, Pharm. Res. 31 (2014) 2393–2403.
[24] M.G. McGrath, S. Vucen, A. Vrdoljak, A. Kelly, C. O'Mahony, A.M. Crean, A. Moore, Production of dissolvable microneedles using an atomised spray process: effect of microneedle composition on skin penetration, Eur. J. Pharm. Biopharm. 86 (2014) 200–211.
[25] M. Dul, M. Stefanidou, P. Porta, J. Serve, C. O'Mahony, B. Malissen, S. Henri, Y. Levin, E. Kochba, F.S. Wong, C. Dayan, S.A. Coulman, J.C. Birchall, Hydrodynamic gene delivery in human skin using a hollow microneedle device, J. Control. Release 265 (2017) 120–131.
[26] Y. Qiu, L. Guo, S. Zhang, B. Xu, Y. Gao, Y. Hu, J. Hou, B. Bai, H. Shen, P. Mao, DNA-based vaccination against hepatitis B virus using dissolving microneedle arrays adjuvanted by cationic liposomes and CpG ODN, Drug Deliv. 23 (2016) 2391–2398.
[27] A. Vrdoljak, E.A. Allen, F. Ferrara, N.J. Temperton, A.M. Crean, A.C. Moore, Induction of broad immunity by thermostabilised vaccines incorporated in dissolvable microneedles using novel fabrication methods, J. Control. Release 225 (2016) 192–204.
[28] G.A. Simon, H.I. Maibach, The pig as an experimental animal model of percutaneous permeation in man: qualitative and quantitative observations–an overview, Skin Pharmacol. Appl. Ski. Physiol. 13 (2000) 229–234.
[29] F. Marquet, T.P. Vu Manh, P. Maisonnasse, J. Elhmouzi-Younes, C. Urien, E. Bouguyon, L. Jouneau, M. Bourge, G. Simon, A. Ezquerra, J. Lecardonnel, M. Bonneau, M. Dalod, I. Schwartz-Cornil, N. Bertho, Pig skin includes dendritic cell subsets transcriptomically related to human CD1a and CD14 dendritic cells presenting different migrating behaviors and T cell activation capacities, J. Immunol. 193 (2014) 5883–5893.

[30] J.K. Lunney, Y. Fang, A. Ladinig, N. Chen, Y. Li, B. Rowland, G.J. Renukaradhya, Porcine reproductive and respiratory syndrome virus (PRRSV): pathogenesis and interaction with the immune system, Annu. Rev. Anim. Biosci. 4 (2016) 129–154.
[31] A. Kumar, P. Wonganan, M.A. Sandoval, X. Li, S. Zhu, Z. Cui, Microneedle-mediated transcutaneous immunization with plasmid DNA coated on cationic PLGA nanoparticles, J. Control. Release 163 (2012) 230–239.
[32] C.M. Barbon, L. Baker, C. Lajoie, U. Ramstedt, M.L. Hedley, T.M. Luby, In vivo electroporation enhances the potency of poly-lactide co-glycolide (PLG) plasmid DNA immunization, Vaccine 28 (2010) 7852–7864.
[33] B. Delmas, J. Gelfi, R. L'Haridon, L.K. Vogel, H. Sjostrom, O. Noren, H. Laude, Aminopeptidase N is a major receptor for the entero-pathogenic coronavirus TGEV, Nature 357 (1992) 417–420.
[34] C. Somasundaram, H. Takamatsu, C. Andreoni, J.C. Audonnet, L. Fischer, F. Lefevre, B. Charley, Enhanced protective response and immuno-adjuvant effects of porcine GM-CSF on DNA vaccination of pigs against Aujeszky's disease virus, Vet. Immunol. Immunopathol. 70 (1999) 277–287.
[35] S. Subramaniam, P. Pineyro, D. Tian, C. Overend, D.M. Yugo, S.R. Matzinger, A.J. Rogers, M.E. Haac, Q. Cao, C.L. Heffron, N. Catanzaro, S.P. Kenney, Y.W. Huang, T. Opriessnig, X.J. Meng, In vivo targeting of porcine reproductive and respiratory syndrome virus antigen through porcine DC-SIGN to dendritic cells elicits antigen-specific CD4T cell immunity in pigs, Vaccine 32 (2014) 6768–6775.
[36] C. Bernelin-Cottet, C. Deloizy, O. Stanek, C. Barc, E. Bouguyon, C. Urien, O. Boulesteix, J. Pezant, C.A. Richard, M. Moudjou, B. Da Costa, L. Jouneau, C. Chevalier, C. Leclerc, P. Sebo, N. Bertho, I. Schwartz-Cornil, A universal influenza vaccine can Lead to disease exacerbation or viral control depending on delivery strategies, Front. Immunol. 7 (2016) 641.
[37] T. Chrun, S. Lacote, C. Urien, L. Jouneau, C. Barc, E. Bouguyon, V. Contreras, A. Ferrier-Rembert, C.N. Peyrefitte, N. Busquets, E. Vidal, J. Pujols, P. Marianneau, I. Schwartz-Cornil, A Rift Valley fever virus Gn ectodomain-based DNA vaccine induces a partial protection not improved by APC targeting, NPJ Vaccines 3 (2018) 14.
[38] P. Maisonnasse, E. Bouguyon, G. Piton, A. Ezquerra, C. Urien, C. Deloizy, M. Bourge, J.J. Leplat, G. Simon, C. Chevalier, S. Vincent-Naulleau, E. Crisci, M. Montoya, I. Schwartz-Cornil, N. Bertho, The respiratory DC/macrophage network at steady-state and upon influenza infection in the swine biomedical model, Mucosal Immunol. 9 (2016) 835–849.
[39] G. Grodeland, A.B. Fredriksen, G.A. Loset, E. Vikse, L. Fugger, B. Bogen, Antigen targeting to human HLA class II molecules increases efficacy of DNA vaccination, J. Immunol. 197 (2016) 3575–3585.
[40] A. Vrdoljak, M.G. McGrath, J.B. Carey, S.J. Draper, A.V. Hill, C. O'Mahony, A.M. Crean, A.C. Moore, Coated microneedle arrays for transcutaneous delivery of live virus vaccines, J. Control. Release 159 (2012) 34–42.
[41] G. Yan, N. Arelly, N. Farhan, S. Lobo, H. Li, Enhancing DNA delivery into the skin with a motorized microneedle device, Eur. J. Pharm. Sci. 52 (2014) 215–222.
[42] F. Marquet, M. Bonneau, F. Pascale, C. Urien, C. Kang, I. Schwartz-Cornil, N. Bertho, Characterization of dendritic cells subpopulations in skin and afferent lymph in the swine model, PLoS One 6 (2011) e16320.
[43] G. Auray, I. Keller, S. Python, M. Gerber, R. Bruggmann, N. Ruggli, A. Summerfield, Characterization and Transcriptomic analysis of porcine blood conventional and Plasmacytoid dendritic cells reveals striking species-specific differences, J. Immunol. 197 (2016) 4791–4806.
[44] T. Granot, T. Senda, D.J. Carpenter, N. Matsuoka, J. Weiner, C.L. Gordon, M. Miron, B.V. Kumar, A. Griesemer, S.H. Ho, H. Lerner, J.J. Thome, T. Connors, B. Reizis, D.L. Farber, Dendritic cells display subset and tissue-specific maturation dynamics over human life, Immunity 46 (2017) 504–515.
[45] M. Ghosh, B. McAuliffe, J. Subramani, S. Basu, L.H. Shapiro, CD13 regulates dendritic cell cross-presentation and T cell responses by inhibiting receptor-mediated antigen uptake, J. Immunol. 188 (2012) 5489–5499.
[46] S. Subramaniam, P. Pineyro, R.J. Derscheid, D.M. Madson, D.R. Magstadt, X.J. Meng, Dendritic cell-targeted porcine reproductive and respiratory syndrome virus (PRRSV) antigens adjuvanted with polyinosinic-polycytidylic acid (poly (I:C)) induced non-protective immune responses against heterologous type 2 PRRSV challenge in pigs, Vet. Immunol. Immunopathol. 190 (2017) 18–25.
[47] H. Mokhtar, M. Eck, S.B. Morgan, S.E. Essler, J.P. Frossard, N. Ruggli, S.P. Graham, Proteome-wide screening of the European porcine reproductive and respiratory syndrome virus reveals a broad range of T cell antigen reactivity, Vaccine 32 (2014) 6828–6837.
[48] N.C. Ganderup, W. Harvey, J.T. Mortensen, W. Harrouk, The minipig as nonrodent species in toxicology–where are we now? Int. J. Toxicol. 31 (2012) 507–528.
[49] A.K. Andrianov, D.P. DeCollibus, H.A. Gillis, H.H. Kha, A. Marin, M.R. Prausnitz, L.A. Babiuk, H. Townsend, G. Mutwiri, Poly[di(carboxylatophenoxy)phosphazene] is a potent adjuvant for intradermal immunization, Proc. Natl. Acad. Sci. U. S. A. 106 (2009) 18936–18941.
[50] A. Summerfield, F. Meurens, M.E. Ricklin, The immunology of the porcine skin and its value as a model for human skin, Mol. Immunol. 66 (2015) 14–21.
[51] K.H. Mair, C. Sedlak, T. Kaser, A. Pasternak, B. Levast, W. Gerner, A. Saalmuller, A. Summerfield, V. Gerdts, H.L. Wilson, F. Meurens, The porcine innate immune system: an update, Dev. Comp. Immunol. 45 (2014) 321–343.
[52] H.D. Dawson, A.D. Smith, C. Chen, J.F. Urban Jr., An in-depth comparison of the porcine, murine and human inflammasomes; lessons from the porcine genome and transcriptome, Vet. Microbiol. 202 (2017) 2–15.
[53] H.D. Dawson, C. Chen, B. Gaynor, J. Shao, J.F. Urban Jr., The porcine translational research database: a manually curated, genomics and proteomics-based research resource, BMC Genomics 18 (2017) 643.
[54] M.A. Groenen, A.L. Archibald, H. Uenishi, C.K. Tuggle, Y. Takeuchi, M.F. Rothschild, C. Rogel-Gaillard, C. Park, D. Milan, H.J. Megens, S. Li, D.M. Larkin, H. Kim, L.A. Frantz, M. Caccamo, H. Ahn, B.L. Aken, A. Anselmo, C. Anthon, L. Auvil, B. Badaoui, C.W. Beattie, C. Bendixen, D. Berman, F. Blecha, J. Blomberg, L. Bolund, M. Bosse, S. Botti, Z. Bujie, M. Bystrom, B. Capitanu, D. Carvalho-Silva, P. Chardon, C. Chen, R. Cheng, S.H. Choi, W. Chow, R.C. Clark, C. Clee, R.P. Crooijmans, H.D. Dawson, P. Dehais, F. De Sapio, B. Dibbits, N. Drou, Z.Q. Du, K. Eversole, J. Fadista, S. Fairley, T. Faraut, G.J. Faulkner, K.E. Fowler, M. Fredholm, E. Fritz, J.G. Gilbert, E. Giuffra, J. Gorodkin, D.K. Griffin, J.L. Harrow, A. Hayward, K. Howe, Z.L. Hu, S.J. Humphray, T. Hunt, H. Hornshoj, J.T. Jeon, P. Jern, M. Jones, J. Jurka, H. Kanamori, R. Kapetanovic, J. Kim, J.H. Kim, K.W. Kim, T.H. Kim, G. Larson, K. Lee, K.T. Lee, R. Leggett, H.A. Lewin, Y. Li, W. Liu, J.E. Loveland, Y. Lu, J.K. Lunney, J. Ma, O. Madsen, K. Mann, L. Matthews, S. McLaren, T. Morozumi, M.P. Murtaugh, J. Narayan, D.T. Nguyen, P. Ni, S.J. Oh, S. Onteru, F. Panitz, E.W. Park, H.S. Park, G. Pascal, Y. Paudel, M. Perez-Enciso, R. Ramirez-Gonzalez, J.M. Reecy, S. Rodriguez-Zas, G.A. Rohrer, L. Rund, Y. Sang, K. Schachtschneider, J.G. Schraiber, J. Schwartz, L. Scobie, C. Scott, S. Searle, B. Servin, B.R. Southey, G. Sperber, P. Stadler, J.V. Sweedler, H. Tafer, B. Thomsen, R. Wali, J. Wang, J. Wang, S. White, X. Xu, M. Yerle, G. Zhang, J. Zhang, J. S. Zhao, J. Rogers, C. Churcher, L.B. Schook, Analyses of pig genomes provide insight into porcine demography and evolution, Nature, 491 (2012) 393–398.
[55] R. Kapetanovic, L. Fairbairn, D. Beraldi, D.P. Sester, A.L. Archibald, C.K. Tuggle, D.A. Hume, Pig bone marrow-derived macrophages resemble human macrophages in their response to bacterial lipopolysaccharide, J. Immunol. 188 (2012) 3382–3394.
[56] L. Fairbairn, R. Kapetanovic, D.P. Sester, D.A. Hume, The mononuclear phagocyte system of the pig as a model for understanding human innate immunity and disease, J. Leukoc. Biol. 89 (2011) 855–871.
[57] T.W. Prow, X. Chen, N.A. Prow, G.J. Fernando, C.S. Tan, A.P. Raphael, D. Chang, M.P. Ruutu, D.W. Jenkins, A. Pyke, M.L. Crichton, K. Raphaelli, L.Y. Goh, I.H. Frazer, M.S. Roberts, J. Gardner, A.A. Khromykh, A. Suhrbier, R.A. Hall, M.A. Kendall, Nanopatch-targeted skin vaccination against West Nile Virus and Chikungunya virus in mice, Small 6 (2010) 1776–1784.
[58] T.R. Smith, K. Schultheis, W.B. Kiosses, D.H. Amante, J.M. Mendoza, J.C. Stone, J.R. McCoy, N.Y. Sardesai, K.E. Broderick, DNA vaccination strategy targets epidermal dendritic cells, initiating their migration and induction of a host immune response, Mol. Ther. Methods Clin. Dev. 1 (2014) 14054.
[59] D.H. Amante, T.R. Smith, J.M. Mendoza, K. Schultheis, J.R. McCoy, A.S. Khan, N.Y. Sardesai, K.E. Broderick, Skin transfection patterns and expression kinetics of electroporation-enhanced plasmid delivery using the CELLECTRA-3P, a portable next-generation dermal electroporation device, Hum Gene Ther Methods 26 (2015) 134–146.
[60] J. McCaffrey, C.M. McCrudden, A.A. Ali, A.S. Massey, J.W. McBride, M.T. McCrudden, E.M. Vicente-Perez, J.A. Coulter, T. Robson, R.F. Donnelly, H.O. McCarthy, Transcending epithelial and intracellular biological barriers; a prototype DNA delivery device, J. Control. Release 226 (2016) 238–247.
[61] M. Guilliams, L. van de Laar, A Hitchhiker's guide to myeloid cell subsets: practical implementation of a novel mononuclear phagocyte classification system, Front. Immunol. 6 (2015) 406.
[62] A.C. Villani, R. Satija, G. Reynolds, S. Sarkizova, K. Shekhar, J. Fletcher, M. Griesbeck, A. Butler, S. Zheng, S. Lazo, L. Jardine, D. Dixon, E. Stephenson, E. Nilsson, I. Grundberg, D. McDonald, A. Filby, W. Li, P.L. De Jager, O. Rozenblatt-Rosen, A.A. Lane, M. Haniffa, A. Regev, N. Hacohen, Single-cell RNA-seq reveals new types of human blood dendritic cells, monocytes, and progenitors, Science 356 (2017).
[63] M. Otsuka, G. Egawa, K. Kabashima, Uncovering the mysteries of Langerhans cells, inflammatory dendritic epidermal cells, and monocyte-derived Langerhans cell-like cells in the epidermis, Front. Immunol. 9 (2018) 1768.
[64] T.L. Tang-Huau, E. Segura, Human in vivo-differentiated monocyte-derived dendritic cells, Semin. Cell Dev. Biol. 86 (2018) 44–49.
[65] N. Munoz-Wolf, E.C. Lavelle, A guide to IL-1 family cytokines in adjuvanticity, FEBS J. 285 (2018) 2377–2401.
[66] J.B. Carey, F.E. Pearson, A. Vrdoljak, M.G. McGrath, A.M. Crean, P.T. Walsh, T. Doody, C. O'Mahony, A.V. Hill, A.C. Moore, Microneedle array design determines the induction of protective memory CD8+ T cell responses induced by a recombinant live malaria vaccine in mice, PLoS One 6 (2011) e22442.
[67] J.B. Carey, A. Vrdoljak, C. O'Mahony, A.V. Hill, S.J. Draper, A.C. Moore, Microneedle-mediated immunization of an adenovirus-based malaria vaccine enhances antigen-specific antibody immunity and reduces anti-vector responses compared to the intradermal route, Sci. Rep. 4 (2014) 6154.
[68] D. Poirier, F. Renaud, V. Dewar, L. Strodiot, F. Wauters, J. Janimak, T. Shimada, T. Nomura, K. Kabata, K. Kuruma, T. Kusano, M. Sakai, H. Nagasaki, T. Oyamada, Hepatitis B surface antigen incorporated in dissolvable microneedle array patch is antigenic and thermostable, Biomaterials 145 (2017) 256–265.
[69] J. Wang, B. Li, M.X. Wu, Effective and lesion-free cutaneous influenza vaccination, Proc. Natl. Acad. Sci. U. S. A. 112 (2015) 5005–5010.
[70] G.J.P. Fernando, J. Hickling, C.M. Jayashi Flores, P. Griffin, C.D. Anderson, S.R. Skinner, C. Davies, K. Witham, M. Pryor, J. Bodle, S. Rockman, I.H. Frazer, A.H. Forster, Safety, tolerability, acceptability and immunogenicity of an influenza vaccine delivered to human skin by a novel high-density microprojection array patch (Nanopatch), Vaccine 36 (2018) 3779–3788.
[71] M.P. Schon, M. Schon, Imiquimod: mode of action, Br. J. Dermatol. 157 (Suppl. 2) (2007) 8–13.
[72] W. Charerntantanakul, Adjuvants for porcine reproductive and respiratory syndrome virus vaccines, Vet. Immunol. Immunopathol. 129 (2009) 1–13.
[73] V. Le Moigne, R. Cariolet, V. Beven, A. Keranflec'h, A. Jestin, D. Dory, Electroporation improves the immune response induced by a DNA vaccine against pseudorabies virus glycoprotein B in pigs, Res. Vet. Sci. 93 (2012) 1032–1035.

[74] V. Gerdts, A. Jons, B. Makoschey, N. Visser, T.C. Mettenleiter, Protection of pigs against Aujeszky's disease by DNA vaccination, J Gen Virol 78 (Pt 9) (1997) 2139–2146.
[75] D. Dory, M. Remond, V. Beven, R. Cariolet, S. Zientara, A. Jestin, Foot-and-mouth disease virus neutralizing antibodies production induced by pcDNA3 and Sindbis virus based plasmid encoding FMDV P1-2A3C3D in swine, Antivir. Res. 83 (2009) 45–52.
[76] Y. Li, C.M. Stirling, M.S. Denyer, P. Hamblin, G. Hutchings, H.H. Takamatsu, P.V. Barnett, Dramatic improvement in FMD DNA vaccine efficacy and cross-serotype antibody induction in pigs following a protein boost, Vaccine 26 (2008) 2647–2656.
[77] A. Burgara-Estrella, I. Diaz, I.M. Rodriguez-Gomez, S.E. Essler, J. Hernandez, E. Mateu, Predicted peptides from non-structural proteins of porcine reproductive and respiratory syndrome virus are able to induce IFN-gamma and IL-10, Viruses 5 (2013) 663–677.
[78] S.B. Morgan, S.P. Graham, F.J. Salguero, P.J. Sanchez Cordon, H. Mokhtar, J.M. Rebel, E. Weesendorp, K.B. Bodman-Smith, F. Steinbach, J.P. Frossard, Increased pathogenicity of European porcine reproductive and respiratory syndrome virus is associated with enhanced adaptive responses and viral clearance, Vet. Microbiol. 163 (2013) 13–22.
[79] J. Lutz, S. Lazzaro, M. Habbeddine, K.E. Schmidt, P. Baumhof, B.L. Mui, Y.K. Tam, T.D. Madden, M.J. Hope, R. Heidenreich, M. Fotin-Mleczek, Unmodified mRNA in LNPs constitutes a competitive technology for prophylactic vaccines, NPJ Vaccines 2 (2017) 29.
[80] N. Pardi, M.J. Hogan, R.S. Pelc, H. Muramatsu, H. Andersen, C.R. DeMaso, K.A. Dowd, L.L. Sutherland, R.M. Scearce, R. Parks, W. Wagner, A. Granados, J. Greenhouse, M. Walker, E. Willis, J.S. Yu, C.E. McGee, G.D. Sempowski, B.L. Mui, Y.K. Tam, Y.J. Huang, D. Vanlandingham, V.M. Holmes, H. Balachandran, S. Sahu, M. Lifton, S. Higgs, S.E. Hensley, T.D. Madden, M.J. Hope, K. Kariko, S. Santra, B.S. Graham, M.G. Lewis, T.C. Pierson, B.F. Haynes, D. Weissman, Zika virus protection by a single low-dose nucleoside-modified mRNA vaccination, Nature 543 (2017) 248–251.
[81] D.K. Edwards, E. Jasny, H. Yoon, N. Horscroft, B. Schanen, T. Geter, M. Fotin-Mleczek, B. Petsch, V. Wittman, Adjuvant effects of a sequence-engineered mRNA vaccine: translational profiling demonstrates similar human and murine innate response, J. Transl. Med. 15 (2017) 1.